Received: 15 October 2023 | Revised: 14 February 2024 | Accepted: 22 February 2024

DOI: 10.1002/ar.25425

SPECIAL ISSUE ARTICLE

The Anatomical Record WILEY

Tarsals from the Sima de los Huesos Middle Pleistocene site (Atapuerca, Burgos, Spain)

Adrián Pablos[1,2,3,4] | **Juan Luis Arsuaga**[1,3]

[1]Departamento de Geodinámica, Estratigrafía y Paleontología, Universidad Complutense de Madrid, Madrid, Spain

[2]Departamento de Prehistoria y Arqueología, Universidad de Sevilla, Sevilla, Spain

[3]Centro Mixto UCM-ISCIII de Investigación sobre Evolución y Comportamiento Humanos, Madrid, Spain

[4]Centro Nacional de Investigación sobre la Evolución Humana (CENIEH), Burgos, Spain

Correspondence
Adrián Pablos, Departamento de Geodinámica, Estratigrafía y Paleontología, Universidad Complutense de Madrid, Madrid, Spain.
Email: adpablos@ucm.es, adrizaino@yahoo.es

Funding information
MCI/AEI/FEDER, UE, Grant/Award Numbers: PGC2018-093925-B-C33, PGC2018-093925-B-C31; MCIN/AEI/10.13039/501100011033/FEDER, UE, Grant/Award Number: PID2021-122355NB-C31; European Research Council, Grant/Award Number: 949330; Junta de Andalucía, Spain, Grant/Award Number: EMERGIA20_00403; Junta de Castilla y León and Fundación Atapuerca

Abstract

Here, we provide a complete, updated, and illustrated inventory, as well as a comprehensive study, of the tarsals (rearfoot) recovered from the Middle Pleistocene site of Sima de los Huesos (SH, Atapuerca, Spain) in comparison to other *Homo* comparative samples, both extant and fossil. The minimum number of individuals (MNI) estimated from the tarsals has been established as 15, which represents 51.7% of the 29 dental individuals identified within the SH sample. Within the SH hominin foot sample, an exclusive combination of primitive or plesiomorphic and derived or autapomorphic traits can be observed when compared with other *Homo* individuals/populations. Other characters are shared among SH hominins and Neandertals that might represent shared derived or autapomorphic traits for this evolutionary line, and most are likely related to robusticity (e.g., rectangular-like trochlea of the talus, broad calcanei, broad naviculars, and short lateral cuneiforms). Additionally, we observed some exclusive autapomorphic traits in the SH tarsal sample (e.g., narrow head of the talus and short intermediate cuneiforms). A few exclusive traits in SH tarsal remains are even more robust than in Neandertals (e.g., broad lateral malleolar facet in talus, more projected sustentaculum tali, and broad medial cuneiform). These traits could suggest a slightly higher level of gracilization in the tarsal bones of Neandertals compared to the SH sample that is also supported by other anatomical postcranial skeleton elements. Additionally, some paleobiological inferences are made in relation to body size (stature and body mass) and some associations are proposed within the SH sample. In conclusion, the morphology of the SH tarsi confirms an evolutionary relationship of sister groups between this population and Neandertals, probably representing a morphotype similar to the Neandertal ancestors.

KEYWORDS
body size, stature estimation; feet; inventory; Neandertal ancestors

1 | INTRODUCTION

The study of foot fossils is highly relevant in human evolution because the feet are involved in locomotion and weight transmission (Pablos, Gómez-Olivencia, et al., 2013; Sorrentino, Stephens, et al., 2020; Trinkaus, 1975). Furthermore, despite their scarcity, they can serve as proxies for body size reconstructions and offer valuable information regarding taxonomic relationships in the human lineage (Castejón-Molina & Pablos, 2021; Pomeroy et al., 2017; Trinkaus, 1983b).

Very few foot fossils existed in the *Homo* fossil record prior to Neandertals. Additionally, they are geographically and chronologically scattered (Boyle & DeSilva, 2015; Lu et al., 2011; Pablos et al., 2012; Pearson et al., 2008). For a better understanding of the morphological origin of the foot of Neandertals, it is necessary to study Early and Middle Pleistocene *Homo* foot fossils. Although similar to recent *Homo sapiens* in morphology, overall size, proportions, and implied locomotor capabilities, the Neandertal feet are generally more robust. Moreover, some metric and morphological traits distinguish Neandertals and recent *H. sapiens*. Neandertal tarsal bones tend to be larger with large articular surfaces, and their tarsals are wider than recent and fossil *H. sapiens* (Pablos et al., 2019; Pearson et al., 2020; Pomeroy et al., 2017; Rhoads & Trinkaus, 1977; Trinkaus, 2016; Vandermeersch, 1981). The Neandertal talus displays a relatively large trochlea, especially with regard to its lateral malleolar facet. The calcanei are robust with broad sustentaculum tali, and the navicular is broad and robust (Harvati et al., 2013; Pablos et al., 2018; Rhoads & Trinkaus, 1977; Sorrentino, Carlson, et al., 2020; Trinkaus, 1975). Traditionally, these differences have been attributed to greater biomechanical stress and general robustness of the postcranial skeleton in Neandertals (Arsuaga et al., 2015; Trinkaus, 1975). The first representatives of the genus *Homo* had feet that were small, whereas the foot fossils of the Early-Middle Pleistocene are large and robust (Boyle & DeSilva, 2015; Lu et al., 2011; Pablos et al., 2012). This large, robust morphotype is maintained in the Neandertals. Recent *H. sapiens* are gracile in comparison to Neandertals. But they probably descend from robust groups from Africa (Arsuaga et al., 1999; Bonmatí et al., 2010; Di Vincenzo et al., 2015; Simpson et al., 2008), indicating that a strong gracilization process, including the narrowing of the whole foot without a decrease in length, has taken place from the Early Pleistocene to the Holocene (Ryan & Shaw, 2015).

In this work, we present a metric and morphological study, together with a complete graphic and descriptive updated inventory, of the tarsals (rearfoot) from the Middle Pleistocene site of Sima de los Huesos—SH (Atapuerca, Burgos, Spain). More than 7000 human fossils from across the skeleton have been recovered from this site during more than 40 years of excavation and research (Arsuaga et al., 2014, 2015), of which more than 500 belong to the foot (Pablos, 2015). They belonged to a minimum of 29 individuals from both sexes, mostly corresponding to late adolescents or young adults (Bermúdez de Castro et al., 2021). They are closely related to Neandertals, both genetically (Meyer et al., 2014, 2016), and morphologically, in spite of some exclusive or autapomorphic traits present in this Middle Pleistocene population (Arsuaga et al., 2014, 2015; Bermúdez de Castro et al., 2024; Carretero et al., 1997; Gómez-Olivencia & Arsuaga, 2024; Pablos et al., 2017; Pablos & Arsuaga, 2024; Pantoja-Pérez et al., 2015; Rodríguez et al., 2016). It has previously been proposed that the SH sample is phylogenetically related to Neandertals, suggesting that this Middle Pleistocene population, or other similar, could be the paleodeme that gave rise to Neandertals in Europe (Arsuaga et al., 2014, 2015). Thus, the SH population and Neandertals likely represent evolutionary sister groups. All the human remains from SH were found in the lithostratigraphic unit—LU-6 (Aranburu et al., 2017), which has been dated to 430–450 ka (Arsuaga et al., 2014; Demuro et al., 2019). The most likely hypothesis suggests that these skeletons were complete when deposited as an act of intentional funerary behavior of anthropic origin (Arsuaga et al., 1991; Arsuaga, Martínez, Gracia, Carretero, et al., 1997; Sala et al., 2016; Sala, Arsuaga, Pantoja-Pérez, et al., 2015; Sala, Martínez, et al., 2024; Sala, Pantoja-Pérez, et al., 2024). Finally, a proxy of body size will be estimated based on the dimensions of the tarsals.

The state of conservation of the human fossils from the SH site is quite good. However, sometimes they appear fragmented with post-depositional fractures, likely caused by the overlying sediment (Sala, Arsuaga, Martínez, & Gracia-Téllez, 2015). Usually, some refittings are done because of the absence of post-depositional deformation processes. They are fragmented, mixed, and comingled, but not all are associated. From the beginning of the excavation of the site 40 years ago, some associations among different elements have been proposed (Bonmatí et al., 2010; Gómez-Olivencia et al., 2007; Rodríguez et al., 2016). However, the possibility exists that we are associating different elements that are likely from separate individuals. The ongoing excavation may provide new elements in the future that represent a better fit than previous ones, and thus the associations suggested now could slightly change based upon future reviews of the collection.

2 | MATERIALS AND METHODS

More than 500 fossils constitute the SH foot sample, of which 149 are tarsals (Arsuaga et al., 2015; Pablos, 2015; Pablos et al., 2017). They represent nearly the same number of specimens in the entire Neandertal fossil record, and there are many more than are found in the worldwide *Homo* fossil record prior to *H. sapiens* and Neandertals (Pablos, 2015).

2.1 | Comparative samples and variables studied

Several *Homo* fossil samples have been used for metric and morphological comparisons of the SH tarsals (see Arsuaga et al., 2015; Pablos et al., 2012, 2017, 2019; Pomeroy et al., 2017; Trinkaus et al., 2014 for details), mainly focusing on Neandertal and early modern human samples. The data sources are mainly bibliographic, but some original specimens/samples have been measured and studied by the authors (e.g., La Ferrassie, La Chapelle-Aux-Saints, Tabun, Regourdou, Cro-Magnon, Gough's Cave, Abri Pataud, Skhul 9, TD6-*H. antecessor*, etc.). Our fossil *H. sapiens* sample is divided into Middle Paleolithic modern humans (MPMH) and Upper Paleolithic modern humans (UP). The MPMH sample is essentially composed of the MIS 5 fossils from Skhul and Qafzeh (McCown & Keith, 1939; Vandermeersch, 1981). The MIS 6–7 Omo-Kibish 1 specimen is considered to belong to MPMH despite its age of around 233 ka (Pearson et al., 2008; Vidal et al., 2022) and the fact that it exhibits some morphological differences relative to the Late Pleistocene *H. sapiens* (Pablos et al., 2012, 2018; Pearson et al., 2008; Trinkaus, 2005). The UP sample is composed of western Eurasian Upper Paleolithic modern humans (see Pablos et al. (2019) for details). Despite morphological changes throughout this period, especially in stature and body proportions, robusticity and morphology of the leg and foot do not appear to have changed during this time (Trinkaus, 2015; Trinkaus et al., 2017).

When available and appropriate, we have included some Eurasian Middle and Early Pleistocene *Homo* fossils in order to assess possible ancestral patterns of pedal morphology, such as the *Homo* specimens from the Dmanisi, TD6-*H. antecessor*, Omo River, Olduvai, Jinniushan, and Koobi Fora samples; and isolated specimens such as Tianyuan and others. In addition, data from four recent/late Holocene comparative samples are included: the Hamann-Todd Osteological collection from the North American 20th century of known sex (Cleveland Museum of Natural History; $n = 244$), the San Pablo Medieval collection of estimated sex (Universidad de Burgos; $n = 45$), the Medieval Sepúlveda Church collection from Segovia (Universidad Complutense de Madrid; $n = 27$), and the unshod Woodland Amerindian collection of unknown sex from the site of Libben, Ohio (Kent State University; $n = 40$; Trinkaus, 1975). This last comparative modern human sample is used to take into consideration the fact that the footwear use in recent populations might influence foot morphology. All the recent modern human samples are pooled sex samples.

In some of the comparative specimens, the antimeres of a given bone are preserved (e.g., La Ferrassie 1 and 2, Amud 1, Sunghir 1, Tabun 1, and the Shanidar, Skhul, Qafzeh, Dolní Věstonice, and Předmostí samples). In these cases, we averaged the available bilateral measurements to provide a mean value for each individual. This value was calculated to better represent the general morphology of individuals rather than elements. Previous studies have shown that there are no significant differences between the left and right foot bones (Bidmos & Dayal, 2003; Pablos, Gómez-Olivencia, et al., 2013; Saldías et al., 2016). In other cases/sites, the association of individuals is not clear (e.g., Cro-Magnon, Krapina, and Moula Guercy samples); for those sites, we considered the bones separately (but see Trinkaus et al. (2021) for a discussion about Cro-Magnon foot associations).

The anatomical variables studied in the present work are linear measurements used in other studies of foot remains, largely following the Martin system (Bräuer (1988); but see Trinkaus (1975, 1983b, 2016), Pablos et al. (2012, 2014, 2018), Pablos, Martínez, et al. (2013), Sala et al. (2013), Pomeroy et al. (2017) for details). The metrical variables were selected in order to describe the general morphology and articular size of each bone. Some of these variables permit differentiation of Neandertal pedal remains from other samples. Additionally, some of these variables are related to body size (McHenry & Berger, 1998; Pablos, Gómez-Olivencia, et al., 2013). We included a comparative section for anatomical traits (see below), indicating the polarity of the different characters (i.e., plesiomorphic or autapomorphic). This is assessed on the basis of metric dimensions, where we indicated that a trait is different between two populations if there are significant differences in a measurement.

The calculation of the minimum number of individuals (MNI) is estimated by identifying the most frequently occurring element in the sample considering adult and immature individuals separately.

In this work, we refer to exclusive traits as autapomorphic or derived traits that are exclusive to a population/group. On the other hand, the term primitive is used here to refer to plesiomorphic or ancestral traits.

2.2 | Sex and body size (stature and body mass) estimations

We are well aware of the limitations of sex assignment in fossil populations. In spite of this, here we try to make initial and approximate assignments to sex based on general size of the tarsals, despite the dependence on a reference population. For sex assignments, we used similar methods to those used to establish sex from the metatarsals and phalanges from SH (Pablos & Arsuaga, 2024). The method consists of performing a principal component analysis (PCA) on the raw variables of each element. We compared the coordinates of the first factor from PCA, usually related to general size, in males and females from the modern samples, and we found significant differences ($p < 0.05$) between the sexes. In order to try to extrapolate that sexual dimorphism to metatarsals and foot phalanges from SH, we first compared the Neandertal and *H. sapiens* fossils that usually are considered to be of known sex. The male fossils fall within the range of variation of modern males for this first factor, and are significantly different from the modern females. The same pattern occurs with the fossils that are generally considered to be females: they are within the range of variation of modern females and significantly different from the modern males. Furthermore, when applicable, we confirm our results to those obtained from discriminant function analysis (see, e.g., Bidmos et al., 2021; Castejón-Molina & Pablos, 2021; Mountrakis et al., 2010).

We are aware of the difficulty and limitations of using forensic samples to estimate the body size (i.e., stature and body mass) of fossil specimens. Moreover, using regression formulae based on femoral head diameter or bi-iliac breadth is usually preferred (Auerbach & Ruff, 2004). In spite of this, we attempted to estimate these parameters in order to glean insight into the body size of the hominins from SH. In the SH, there are some tibiae and femora that are complete enough to calculate body height (Carretero et al., 2012). However, we provide stature estimations based on the tarsals from SH in order to facilitate comparisons with other Pleistocene sites.

The stature estimates using the SH tarsals are based on the maximum length of talus (M1) and calcaneus (M1) when applying the formulae provided by Pablos, Gómez-Olivencia, et al. (2013). When the sex of the talus and calcaneus is known or can be estimated, sex-specific equations are preferable since these will provide statures with a lower Standard Error of Estimate (SEE) and thus the estimates are more accurate. We applied the male formulae for the male-identified tarsals from SH, the female formulae for the female-identified tarsals, and both male and female formulae for those elements classified as indeterminate. In this last case, we calculated the average male and female values for each bone.

In order to estimate body mass from the SH tali, we applied the formulae of least squares for human-based regression provided by McHenry (1992). The mediolateral breadth of the trochlea (M5) was used to assess the body mass of the SH tali.

2.3 | Statistical and osteometric analysis

A comparative univariate analysis of all variables was carried out. We performed a Kruskal-Wallis test to compare differences between the SH and Neandertal, UP, MPMH, and recent modern human samples. When a significant difference ($p < 0.05$) was found for a variable, we performed a Mann–Whitney test on all possible pairs of samples to determine which pairs were significantly different (Mann & Whitney, 1947). We adjusted the p-values for these comparisons using the Dunn-Sidák method ($1 - (1 - \alpha)^{1/n}$) (Rafter et al., 2002). This method

TABLE 1 Minimum number of individuals established by the tarsals in SH.

				Adult			
Element	**NR**	**MNE**	**MNI**	**Total**	**Male**	**Female**	**Imm**
Talus	26	25	14	11	3	4	3
Calcaneus	30	26	15	9	4	3	6
Navicular	25	25	15	10	3	3	5
Cuboid	23	18	10	7	3	1	3
Medial cuneiform	15	15	9	6	3	1	3
Intermediate cuneiform	16	16	10	8	-	-	2
Lateral cuneiform	14	14	8	6	1	1	2

Note: Sex has been assigned preliminarily based on what was previously proposed by Pablos, Martínez, et al. (2013) and Pablos et al. (2017).

Abbreviations: Imm, immature individuals; MNE, minimum number of elements; MNI, minimum number of individuals established with each anatomical part; NR, number of remains; SH, Sima de los Huesos.

TABLE 2 Mean and standard deviation of the variables of the Sima de los Huesos (SH) tali and calcanei (in mm) and other comparative samples.

		SH	Nea	UP	MPMH	MH-HTH	MH-Lib	MH-SPab
Talus	Talar length—M1	51.7 ± 3.5 [46.7–57.0] (n = 19)	50.9 ± 3.3 [46.0–56.9] (n = 22)	53.3 ± 4.4 [44.8–63.0] (n = 30)	53.3 ± 4.5 [46.9–59.1] (n = 8)	52.8 ± 4.0 [43.9–61.8] (n = 162)	50.5 ± 3.2 [42.7–54.8] (n = 40)	50.5 ± 3.6 [44.2–57.4] (n = 45)
	Post. trochlear breadth—M5-1[2,6]	27.1 ± 2.2 [24.0–32.6] (n = 19)	26.9 ± 2.7 [21.8–31.5] (n = 19)	**24.2 ± 2.2 [20.0–28.5] (n = 12)**	24.4 ± 3.9 [19.0–30.0] (n = 8)	26.1 ± 2.6 [29.9–31.7] (n = 112)	-	**25.6 ± 2.1 [21.3–30.4] (n = 45)**
	Ant. trochlear breadth—M5-2	30.2 ± 2.5 [26.5–35.6] (n = 20)	29.5 ± 2.9 [26.0–33.9] (n = 14)	31.2 ± 2.3 [27.5–35.5] (n = 13)	30.2 ± 3.4 [24.8–35.0] (n = 8)	30.3 ± 2.5 [24.9–35.8] (n = 112)	-	29.6 ± 2.5 [24.7–35.0] (n = 45)
	Lat. malleolar breadth—M7a[1,2,3,4,6]	13.2 ± 1.9 [8.9–16.2] (n = 21)	**10.5 ± 2.5 [7.0–15.6] (n = 18)**	**10.3 ± 1.4 [8.0–12.8] (n = 12)**	**10.8 ± 1.3 [9.0–12.2] (n = 6)**	**9.4 ± 2.2 [2.9–15.1] (n = 112)**	8.9 ± 1.4 [6.5–12.0] (n = 40)	**8.1 ± 1.9 [4.4–13.7] (n = 45)**
	Head–neck length—M8[1,4]	20.4 ± 1.8 [17.3–24.2] (n = 19)	**18.7 ± 2.1 [13.8–22.5] (n = 27)**	21.7 ± 4.1 [14.0–30.6] (n = 22)	19.2 ± 2.3 [15.5–23.0] (n = 7)	**23.1 ± 2.9 [16.3–29.3] (n = 112)**	21.1 ± 1.9 [18.5–25.4] (n = 40)	20.9 ± 2.4 [15.7–27.0] (n = 45)
	Breadth of head—M9[1,2,4,5]	30.5 ± 2.2 [27.4–34.2] (n = 19)	**34.2 ± 3.6 [25.5–38.8] (n = 23)**	**34.2 ± 3.2 [28.0–41.3] (n = 20)**	32.9 ± 3.3 [28.2–36.6] (n = 7)	**32.5 ± 2.9 [23.7–40.6] (n = 161)**	**33.2 ± 2.7 [28.4–39.5] (n = 40)**	31.9 ± 3.0 [25.6–38.0] (n = 44)
Calcaneus	Medial breadth—M2[4,5,6]	44.6 ± 3.0 [39.1–48.8] (n = 14)	44.2 ± 3.4 [38.5–47.5] (n = 13)	43.1 ± 3.0 [37.5–50.5] (n = 28)	44.0 ± 2.2 [40.8–45.9] (n = 4)	**40.0 ± 3.7 [29.6–51.1] (n = 164)**	**40.6 ± 2.9 [32.2–46.7] (n = 40)**	**40.1 ± 2.7 [34.5–46.2] (n = 46)**
	Body length—M5[5,6]	58.3 ± 4.3 [51.6–65.0] (n = 13)	59.7 ± 5.7 [50.8–67.6] (n = 11)	58.0 ± 4.7 [49.8–67.7] (n = 21)	58.0 [55.0–60.0] (n = 3)	56.7 ± 4.6 [42.8–69.5] (n = 164)	**53.9 ± 3.6 [46.6–61.0] (n = 40)**	**54.1 ± 4.1 [47.5–68.7] (n = 46)**
	Sustentacular breadth—M6[1,2,3,4,5,6]	17.6 ± 2.4 [12.7–21.3] (n = 14)	**15.2 ± 3.3 [9.6–21.0] (n = 13)**	**14.6 ± 2.5 [9.2–18.6] (n = 22)**	**13.6 ± 1.3 [11.5–15.0] (n = 5)**	**14.2 ± 2.6 [9.5–24.1] (n = 114)**	**12.6 ± 1.8 [9.1–17.7] (n = 40)**	**11.8 ± 1.8 [8.1–16.9] (n = 46)**

Note: Mean ± standard deviation, range [ ], and sample size (n) are shown. Bold letters and superscript indicate significant differences between SH with some of the samples (Z-score >1.96 in absolute terms; $p < 0.05$); 1 = Neandertals, 2 = UP, 3 = MPMH, 4 = Recent modern humans (HTOC-HTH), 5 = Recent modern humans (Libben Amerindians), 6 = Recent modern humans (San Pablo Medieval collection). Nea = Neandertals. MPMH = Middle Paleolithic Modern Humans. UP = Upper Paleolithic Modern Humans. MH-HTH = Modern humans; Hamann-Todd Osteological collection. MH-Lib = Modern humans; Libben, Amerindians unshod (Trinkaus, 1975). MH-SPab = Modern humans; San Pablo Medieval collection. See Pablos, Martínez, et al. (2013), Pablos et al. (2014, 2019), for the sample composition.

TABLE 3 Mean and standard deviation of the variables of the Sima de los Huesos (SH) anterior tarsals (in mm) and other comparative samples.

		SH	Nea	UP	MPMH	MH-HTH	MH-Lib	MH-SPab
Navicular	Maximum breadth—M1[2,4,5,6]	44.1 ± 3.8 [37.6–50.2] ($n = 10$)	43.9 ± 3.0 [38.9–47.7] ($n = 13$)	**39.6 ± 3.3 [34.6–45.0] ($n = 21$)**	39.6 ± 3.8 [35.7–46.7] ($n = 6$)	**40.0 ± 3.2 [32.4–46.4] ($n = 111$)**	**37.9 ± 2.3 [31.8–41.2] ($n = 40$)**	**38.3 ± 2.9 [32.9–43.6] ($n = 41$)**
	Maximum height—M2	26.0 ± 2.1 [22.5–29.6] ($n = 17$)	27.9 ± 2.3 [24.0–33.3] ($n = 13$)	28.1 ± 2.7 [24.1–34.5] ($n = 22$)	26.4 ± 1.6 [24.0–28.1] ($n = 5$)	27.4 ± 3.1 [20.4–38.0] ($n = 112$)	26.2 ± 1.8 [23.4–31.1] ($n = 40$)	26.6 ± 2.5 [21.8–34.1] ($n = 44$)
Cuboid	Medial dorsal length—M1[2,4,5,6]	26.8 ± 2.3 [23.8–30.9] ($n = 14$)	27.1 ± 3.1 [20.6–31.3] ($n = 10$)	**32.1 ± 3.9 [25.5–41.4] ($n = 19$)**	26.6 ($n = 2$)	**30.3 ± 2.7 [23.9–36.3] ($n = 113$)**	**28.6 ± 1.9 [23.7–32.8] ($n = 39$)**	**28.8 ± 2.9 [21.5–35.9] ($n = 45$)**
	Proximal breadth—T2	26.8 ± 2.7 [21.9–30.0] ($n = 10$)	27.8 ± 3.7 [24.2–34.5] ($n = 7$)	30.1 ± 2.2 [26.9–31.7] ($n = 4$)	23.9 ($n = 1$)	28.8 ± 2.8 [22.5–36.8] ($n = 113$)	-	28.1 ± 2.4 [23.6–33.3] ($n = 45$)
Medial cuneiform	Inferior length—M1	26.2 ± 1.2 [24.1–27.1] ($n = 7$)	24.9 ± 2.1 [21.8–27.2] ($n = 7$)	25.8 ± 1.8 [23.3–29.4] ($n = 17$)	23.5 ± 1.9 [21.2–27.5] ($n = 7$)	26.4 ± 2.1 [22.0–32.8] ($n = 113$)	25.0 ± 1.8 [21.2–29.1] ($n = 40$)	25.0 ± 2.0 [21.7–30.3] ($n = 46$)
	Plantar breadth—T11[3,4,5,6]	20.8 ± 1.2 [19.9–22.4] ($n = 5$)	18.7 ± 2.6 [15.0–21.6] ($n = 7$)	18.0 ± 1.8 [16.0–20.1] ($n = 4$)	**18.0 ± 0.8 [17.0–18.9] ($n = 4$)**	**18.6 ± 1.7 [14.5–23.9] ($n = 113$)**	**17.7 ± 2.8 [13.4–32.8] ($n = 40$)**	**18.1 ± 1.6 [14.7–21.5] ($n = 46$)**
Intermediate cuneiform	Superior length—M1[1,2,4,5,6]	15.4 ± 0.9 [13.7–17.1] ($n = 13$)	**16.8 ± 1.2 [15.4–18.9] ($n = 11$)**	**17.3 ± 1.9 [13.7–21.9] ($n = 20$)**	15.2 ± 0.6 [14.7–15.9] ($n = 4$)	**17.5 ± 1.7 [13.6–21.8] ($n = 112$)**	**17.1 ± 1.1 [15.1–19.5] ($n = 40$)**	**17.5 ± 1.6 [14.9–21.3] ($n = 40$)**
Lateral cuneiform	Superior length—M1[2,3,4,6]	18.2 ± 1.7 [16.3–21.8] ($n = 9$)	19.9 ± 2.3 [17.0–22.9] ($n = 12$)	**22.8 ± 2.8 [18.0–28.2] ($n = 31$)**	**20.1 ± 0.5 [19.5–20.7] ($n = 4$)**	**20.9 ± 1.8 [15.9–25.9] ($n = 112$)**	-	**20.1 ± 1.7 [16.9–24.5] ($n = 44$)**

Note: Mean ± standard deviation, range [ ], and sample size (n) are shown. Bold letters and superscript indicate significant differences between SH with some of the samples (Z-score >1.96 in absolute terms; $p < 0.05$); 1 = Neandertals, 2 = UP, 3 = MPMH, 4 = Recent modern humans (HTOC-HTH), 5 = Recent modern humans (Libben Amerindians), 6 = Recent modern humans (San Pablo Medieval collection). SH = Sima de los Huesos. Nea = Neandertals. MPMH = Middle Paleolithic Modern Humans. UP = Upper Paleolithic Modern Humans. MH-HTH = Modern humans; Hamann-Todd Osteological collection. MH-Lib = Modern humans; Libben, Amerindians unshod (Trinkaus, 1975). MH-SPab = Modern humans; San Pablo Medieval collection. See Pablos, Martínez, et al. (2013), Pablos et al. (2014, 2019), for the sample composition.

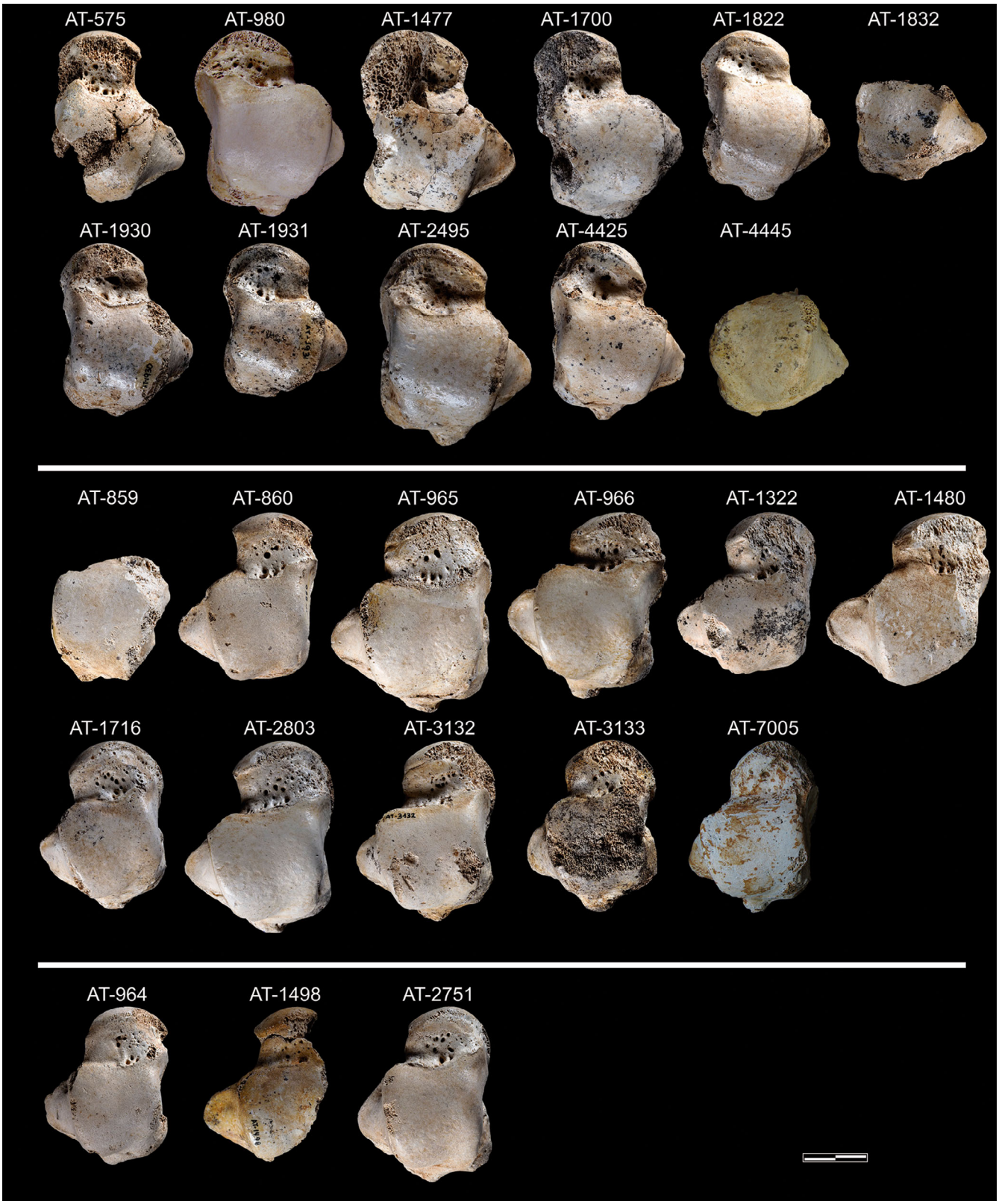

FIGURE 1 Representation of some of the hominin tali from Sima de los Huesos including complete right adult bones (upper rows), complete left adult bones (intermediate rows), and immature tali (lower row) in Dorsal view. Scale bar = 2 cm. See Table 4 for details about the identification.

TABLE 4 Inventory of Tali from SH.

Label	Side	Age	Anatomical description
AT-575	R	Ad	Nearly complete with an oblique fracture with erosion and the resulting exposure of cancellous bone.
AT-859	L	Ad	Trochlear fragment. It preserves a small fragment of the posterior calcaneal facet and the *flexor hallucis longus* groove.
AT-860	L	Ad	Complete. Slight erosion of the articular facets especially on the posterior calcaneal facet and the head.
AT-964	L	Im	Complete. Slight erosion at the edges of the articular surfaces.
AT-965	L	Ad	Complete. Slight erosion at the edges of the articular surfaces.
AT-966[a]	R	Ad	Complete.
AT-980[a]	L	Ad	Complete.
AT-1322	L	Ad	Nearly complete. It displays some erosion on the posterior calcaneal facet and on the head.
AT-1477	R	Ad	Nearly complete. It consists of at least seven fragments with a marked erosion and loss of internal spongy bone tissue.
AT-1480	L	Ad	Quite complete. Longitudinal fracture with spongy bone tissue exposed.
AT-1498	L	Im	Lateral half. Longitudinal fracture with spongy bone tissue exposed.
AT-1700	R	Ad	Nearly complete. It presents furrowing in the medial zone of the trochlea.
AT-1716	L	Ad	Complete.
AT-1822	R	Ad	Complete. Slight erosion at the vertices of the articular facets of the head and trochlea.
AT-1832	R	Ad	Posterior half of talus (trochlea).
AT-1930	R	Ad	Complete. Slight erosion on the posterior side.
AT-1931	R	Ad	Complete. It displays deformation of the upper zone of the trochlea and slight erosion at the edges of the articular facets.
AT-2495	R	Ad	Complete.
AT-2751	L	Im	Complete.
AT-2803	L	Ad	Complete.
AT-2844	L?	?	Head fragment.
AT-3132	L	Ad	Complete with slight erosion in the plantar and dorsal zone of the head.
AT-3133	L	Ad	Complete. Marked erosion of the trochlea and head which largely exposes trabecular tissue.
AT-4425	R	Ad	Complete. Displays slight erosion of the margins of the articular surface of the head.
AT-4445	R	Ad	Posterior half of talus (trochlea).
AT-7005	L	Ad	Complete with slight erosion. A generalized crust is visible on all the bone.

Note: L = left. R = Right. Ad = Adult. Im = Immature. Updated from Pablos, Martínez, et al. (2013).
Abbreviation: SH, Sima de los Huesos.
[a]These tali belong to the same individual (Lorenzo et al., 1998; Pablos et al., 2017).

established a new threshold for the significance level at $p < 0.025$. To compare individual values with the averages from the different samples, *Z*-scores were calculated when the comparative sample size was ≥4, and a value of 1.96 was considered significant ($p < 0.05$; Sokal & Rohlf, 2003).

3 | RESULTS

In general, the SH tarsal collection displays both complete bones and fragments in different stages of preservation corresponding to both juvenile and adult individuals. Over more than 40 years of excavation and laboratory work, some of the fragments are glued together to make complete bones (e.g., the cranium and other postcranial bones; Arsuaga et al., 2014, 2015; Bonmatí et al., 2010; Gómez-Olivencia et al., 2007; Pablos & Arsuaga, 2024; Pantoja-Pérez et al., 2016; Rodríguez et al., 2016). The tarsals sometimes also underwent this gluing process, as indicated below.

The SH tarsals from SH correspond to a minimum number of 15 individuals (Table 1), which correspond to 51.7% of the total 29 individuals established using the dental remains (Bermúdez de Castro et al., 2021). Tables 2 and 3 provide a summary of the statistics for the SH and comparative samples of the main variables considered in this study.

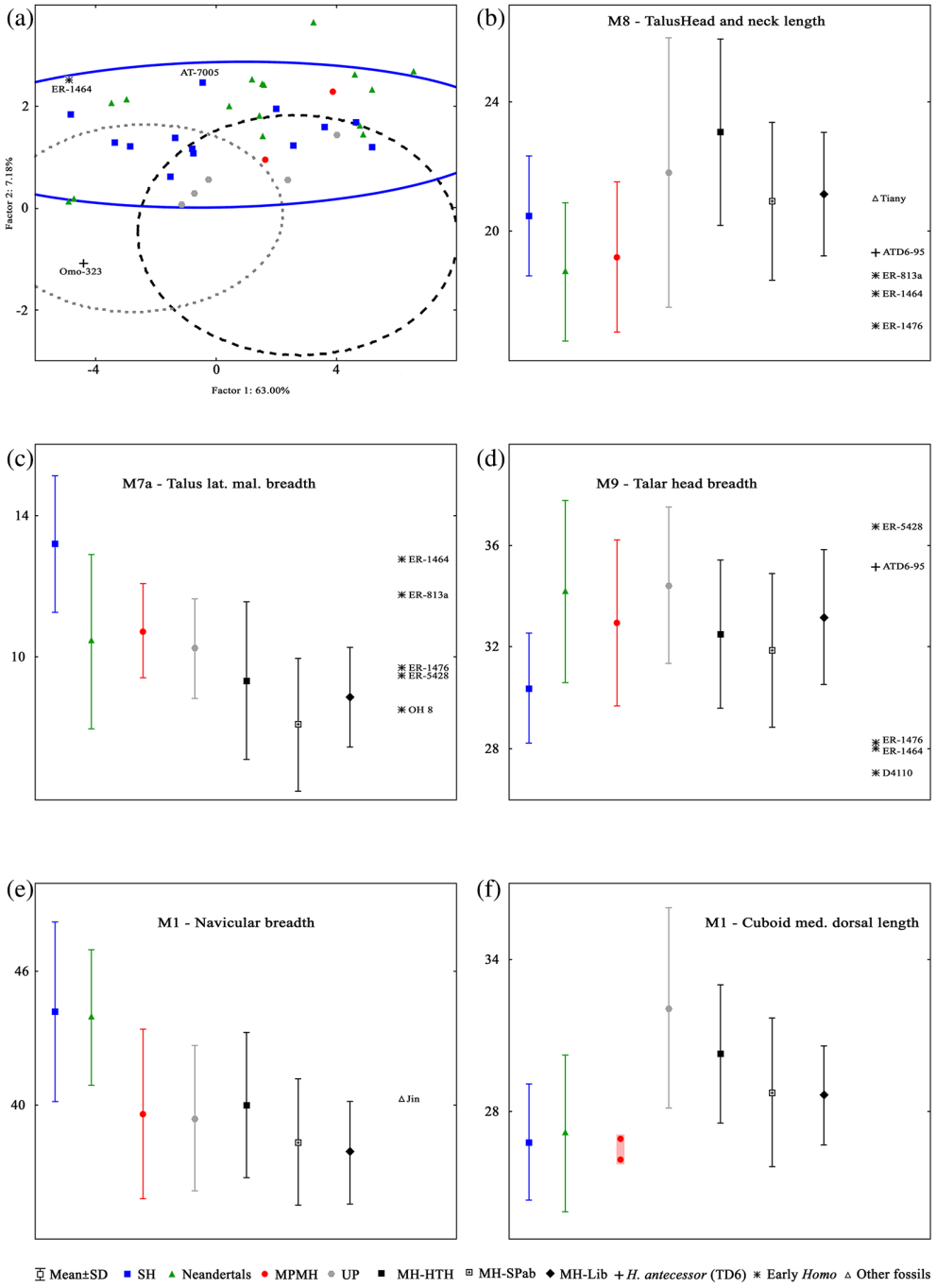

FIGURE 2 (a) Scatter diagram based on principal component analysis (PCA) for first and second factors of talus variables. The dashed line indicates the 95% equiprobability ellipse of modern human (MH) variation, males ($n = 76$) and females ($n = 78$). The solid blue ellipse indicates 95% of the Sima de los Huesos (SH) variation. The *x*-axis and *y*-axis show the factors and their percentage of variance, respectively. The Neandertal sample (Nea) includes: Amud 1 left, Kiik-Koba 1 right and left, Krapina 235, La Chapelle-aux-Saints 1, La Ferrassie 1 right and left; La Ferrassie 2 left, La Quina 1 right and left, Regourdou 1 right and left, Shanidar 5 right, Spy 2 left, and Tabun C1 right and left. The Middle Paleolithic modern human sample (MPMH) includes Skhul 4 left and Skhul 5 left. The Upper Paleolithic modern human sample (UP) includes Abri Pataud right and left, Cro-Magnon 4337 left and 438 right, and Gough's Cave 1 right. (b) Talus head–neck length (in mm). Univariate analysis of the tarsal remains from the SH sample. SD, standard deviation. (c) Talus lateral malleolar breadth (in mm). (d) Talar head breadth (in mm). (e) Navicular breadth (in mm). (f) Dorsal length of the cuboid (in mm). MH-HTH, Modern humans-Hamann-Todd Osteological collection; MH-Lib, Modern Humans-Libben-Amerindians collection (unshod); MH-SPab, Modern humans-Medieval. See Trinkaus (1975, 2016), Pablos et al. (2012, 2014, 2017, 2018, 2019), Pablos, Martínez, et al. (2013), Sala et al. (2013), Trinkaus et al. (2014), Pomeroy et al. (2017), and Pearson et al. (2020) for the composition of the samples and description of the variables. Tiany, Tianyuan; Jin, Jinniushan.

3.1 | Talus

There are 26 talus fragments in the SH site corresponding to a minimum of 25 elements and 14 individuals (Arsuaga et al., 2015), represented by 11 adults and three juveniles (Table 1 and Figure 1). The complete inventory of tali from SH is displayed in Table 4.

The general morphology of the talus has not changed much in genus *Homo* over the last 1.5–1.6 ma (Boyle & DeSilva, 2015; Pablos et al., 2012; Pablos, Martínez, et al., 2013; Pearson et al., 2020; Trinkaus, 2016). In general, the Neandertal tali are indistinguishable from those of *H. sapiens* in their implied locomotor capabilities and similar in overall size and proportions. However, they tend to have relatively larger articular surfaces than those of *H. sapiens*, for example, in the lateral malleolar facet and the head (Rhoads & Trinkaus, 1977; Sorrentino et al., 2021; Trinkaus, 1975, 1983b). Generally, the fossil tali not belonging to *H. sapiens* display a short neck that differentiates them from recent modern humans (Figure 2b). The Neandertal talus displays a broad lateral malleolar facet compared to recent modern humans, and a very broad head (Gómez-Olivencia et al., 2020; Pablos et al., 2019; Pearson et al., 2020; Rhoads & Trinkaus, 1977).

The talus bones from SH display metrical variables similar to Neandertals, for example, a trochlear wedging index that indicates a more rectangular trochlea in SH and Neandertals compared to fossil *H. sapiens*. However, the lateral malleolar facet, already significantly broad in Neandertals, is even broader in SH than in Neandertals (Table 2 and Figure 2c). The lateral malleolar facet may be broad in SH and Neandertals likely due to a talocrural stabilization or a slight lateral shift in forces through the ankle. In the tali, KNM-ER 813a and KNM-ER 1464, supposedly belonging to *H. ergaster*, the lateral malleolar facet is slightly broad (Figure 2c). The Early Pleistocene

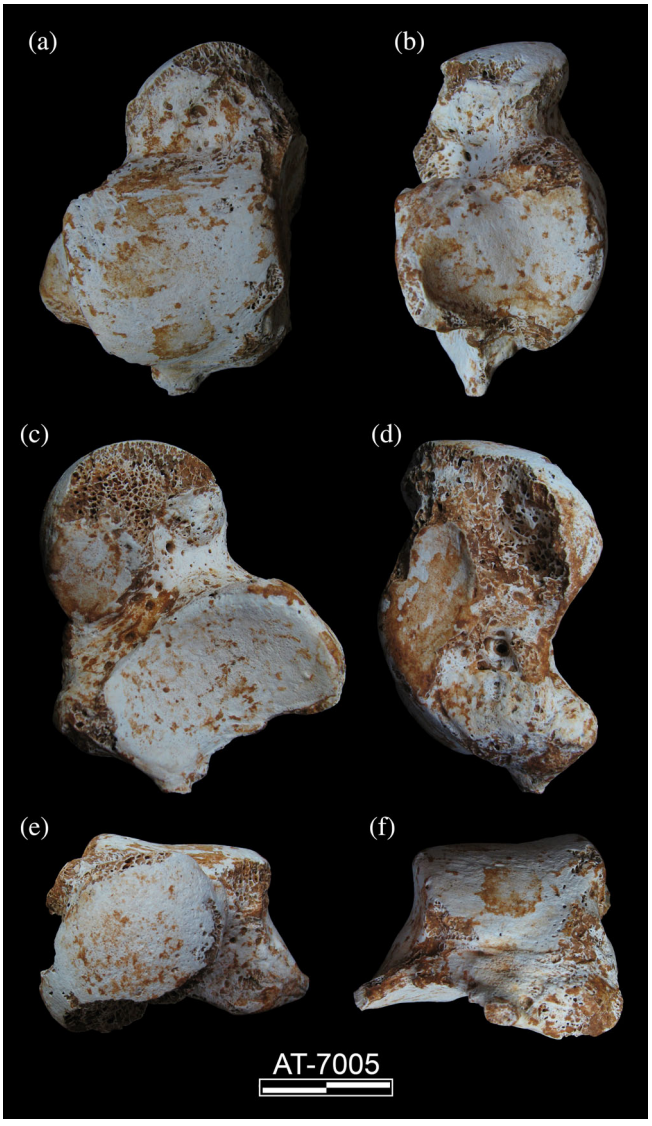

FIGURE 3 AT-7005. Left talus. Views: (a) dorsal, (b) lateral, (c) plantar, (d) medial, (e) anterior, and (f) posterior.

TABLE 5 AT-7005 metrical measurements (in mm).

	AT-7005
Talar length—M1	48.4
Total length—M1a	53.3
Total breadth—M2	43.2
Articular breadth—M2b	43.2
Talar height—M3	26.0
Medial height—M3-1	27.7
Trochlear length—M4	32.0
Trochlear breadth—M5	28.9
Posterior trochlear breadth—M5-1	27.7
Anterior trochlear breadth—M5-2	29.8
Lateral malleolar oblique height—M7	24.3
Lateral malleolar breadth—M7a	13.7
Head–neck length—M8	19.6
Length of the head—M9	32.6
Breadth of the head—M10	21.9
Length of calcaneal post. artic. surf.—M12	32.0
Breadth of calcaneal post. artic. surf.—M13	21.3
Depth of calcaneal post. artic. surf.—M14	7.5
Lateral malleolar length—D4	29.2
Breadth of calcaneal middle artic. surf.—E2	13.5
Lateral height—L2	26.5
Medial malleolar length—L13	28.5
Lateral malleolar height—T6	22.5

Note: For a description of the variables, see Pablos, Martínez, et al. (2013).

talus ATD6-95 belonging to *H. antecessor* (Pablos et al., 2012) is large and displays a long, wide, and high trochlea. The taphonomic erosion of this specimen makes the lateral malleolar facet unavailable to study this character.

Another trait differentiating SH and Neandertals is the narrow head in SH tali (Pablos et al., 2017; Pablos, Martínez, et al., 2013). The Neandertal tali have a significantly broad head, whereas the SH tali have a significantly narrow head (Figure 2d). Talar length shows a similar pattern. In SH, the longer the talus is, the narrower the head. However, in Neandertals, the longer the talus is, the broader the head (Pablos et al., 2017).

From the last updated inventory from SH (Pablos et al., 2017) a new complete talus has been found in recent field campaigns in the SH site labeled as AT-7005 (Figure 3). It corresponds to an adult talus from the left side with slight erosion in the plantar area. The metrical dimensions of this new talus fall comfortably inside the SH range of variation, and it shows a very broad lateral malleolar facet (Table 5). In order to assess morphological similarities between the talus AT-7005 and comparative samples, we performed a PCA on the raw variables with those samples and specimens that possess the same variables as talus AT-7005. Table 6 shows the factor matrix of this PCA and the loadings of the variables on the factors. There are only two factors with an eigenvalue greater than 1, which together account for 70.18% of the total variance. All of the variables are positively correlated with the first factor, and except in three cases (M7a, M8, and M14), all of the variables have a correlation greater than 0.6 with the first factor. Despite the fact that there is no clear correlation with the geometric mean (size proxy), the first factor could be considered a factor for the general size of the talus. Factor 1 accounts for 63% of the variance. In this way, the largest talus bones have high positive values, and the smallest tali have high negative values. The second factor is correlated mainly with the lateral malleolar breadth (M7a). Unlike the first factor, the second is bipolar, with some variables with negative loadings and others with positive loadings. However, and although with a lower correlation (load = −0.521), the depth of the calcaneal posterior articular surface (M14) offers a negative load. This second factor can be considered a factor for shape, in which tali with a wide lateral malleolar breadth and a small depth of the calcaneal posterior articular surface will have high positive values.

When the first principal component is plotted against the second (Figure 2a) several interesting conclusions can be drawn. Most of the fossil tali show values in the PCA that fall comfortably within the range of variation of recent *H. sapiens*. The second factor of PCA-1 has some taxonomic value. Nearly all the fossils display positive values for the second factor, which positions them among the tali with broad lateral malleolar facets and small depths of the calcaneal posterior articular surface from the modern human sample. The recent *H. sapiens* display positive and negative values independent of their a priori sex assignment. In the comparison of the first factor, there are no significant differences among the different comparative populations. When comparing the second factor, there are significant differences between SH and all the groups including Neandertals. Neandertals also show significant differences with recent *H. sapiens* and Upper Paleolithic modern humans (UP).

The specimen AT-7005 shows a particularly high positive value for the second factor, which indicates a broad lateral malleolar facet and a shallow calcaneal posterior articular surface. It is inside the range of variation of SH tali and outside of the range of variation of the equiprobability ellipses of recent *H. sapiens* (Figure 2a).

TABLE 6 Principal component analysis of the AT-7005 talus variables.

	Factor 1	Factor 2
Eigenvalue	10.71	1.22
% Variance	63.00	7.18
% Cumulative Variance	63.00	70.18
Talar length—M1	**0.921**	−0.192
Total length—M1a	**0.900**	−0.189
Total breadth—M2	**0.899**	0.271
Articular breadth—M2b	**0.885**	0.285
Talar height—M3	**0.636**	−0.049
Medial height—M3-1	**0.885**	−0.021
Trochlear length—M4	**0.842**	0.006
Trochlear breadth—M5	**0.897**	−0.114
Posterior trochlear breadth—M5-1	**0.829**	0.041
Anterior trochlear breadth—M5-2	**0.909**	−0.079
Lateral malleolar breadth—M7a	0.304	**0.749**
Head–neck length—M8	0.594	−0.330
Length of the head—M9	**0.815**	0.155
Breadth of the head—M10	**0.764**	0.065
Length of calcaneal post. artic. surf.—M12	**0.853**	0.022
Breadth of calcaneal post. artic. surf.—M13	**0.823**	0.010
Depth of calcaneal post. artic. surf.—M14	0.380	−0.521

Note: Loadings above 0.6 (absolute value) are highlighted (bold).

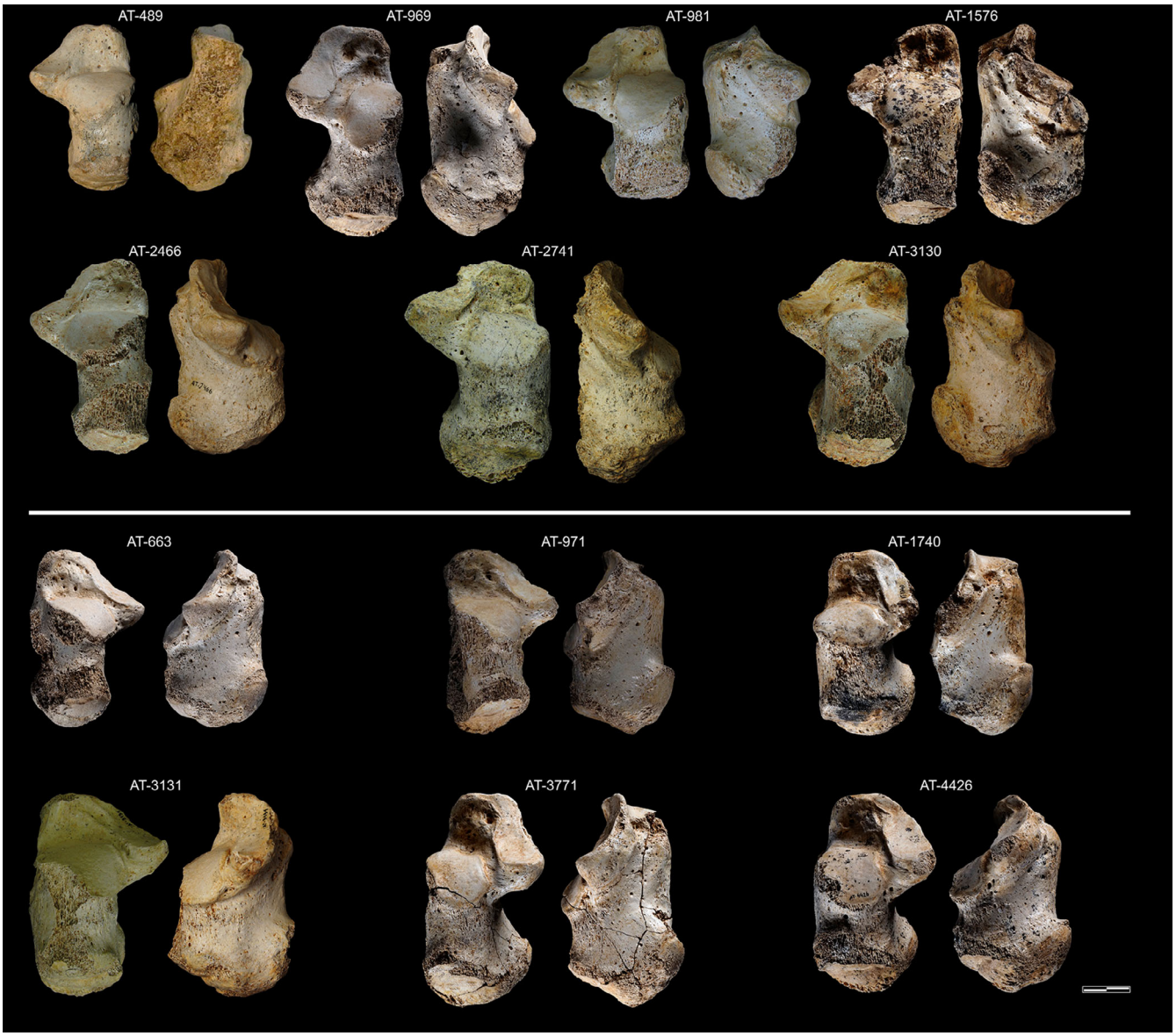

FIGURE 4 Representation of some of the adult calcanei from Sima de los Huesos including right bones and left bones in dorsal and medial views. Scale bar = 2 cm. See Table 7 for details about the identification.

In order to gain some insights into the paleobiology of this Middle Pleistocene population, we tried to estimate sex based on the overall size of the fossils in general, and for AT-7005 in particular, despite the dependence on a reference population (see Pablos, Martínez, et al., 2013, for details about the methodology). This method allowed us to estimate the sex of the previously known SH tali (Pablos, Martínez, et al., 2013).

When we compared the coordinates of the first factor of the PCA of the recently discovered talus AT-7005 using the *Z*-scores statistics with recent modern males, no significant differences were observed. However, it is 1.9 standard deviations away from the sample of recent modern human males from the Hamann-Todd Osteological collection. In the comparisons with the male tali from SH, AT-7005 is more than two standard deviations away. In the comparisons with the female groups, it only show significant differences with the female Neandertals. However, the small sample size ($n = 4$) of this group precludes any firm conclusions. All this suggests that the talus AT-7005 could correspond to a female individual.

To clarify the sex estimation of the talus AT-7005, we applied the univariate discriminant equations obtained by Alonso-Llamazares and Pablos (2019) for recent modern human tali. Eight univariate equations could be applied to the metric variables of AT-7005. The results classified AT-7005 as male for four variables and female for four others. We then applied multivariate discriminant equations from different bibliographic sources and populations (Alonso-Llamazares & Pablos, 2019; Bidmos &

Dayal, 2003; Gualdi-Russo, 2007; Mahakkanukrauh et al., 2014; Peckmann et al., 2015; Steele, 1976). In this case, the talus AT-7005 was identified as female using 12 equations, and as male in four cases. With these results, we cautiously established the sex of AT-7005 as female.

3.2 | Calcaneus

In the SH site, there are 30 calcanei corresponding to complete and fragmentary remains (Figures 4 and 5). They represent at least 26 elements and 15 individuals based on the most repeated element (i.e., the intermediate talar facet) and the stage of development (Pablos et al., 2014). The calcaneal individuals represent nine adults and six immatures (Table 1). The detailed inventory of SH calcanei is shown in Table 7. Three calcanei from SH (AT-970, AT-3269, and AT-967) have the posterior calcaneal tubercle partially fused. According to Cardoso and Severino (2010), this corresponds to stage 2 indicating they were in the age range of 11–17 years at the time of death.

The general morphology of the Neandertal calcanei is indistinguishable from that of *H. sapiens* in terms of the implied locomotor capabilities. They have large articular surfaces, and they are characterized by being mediolaterally

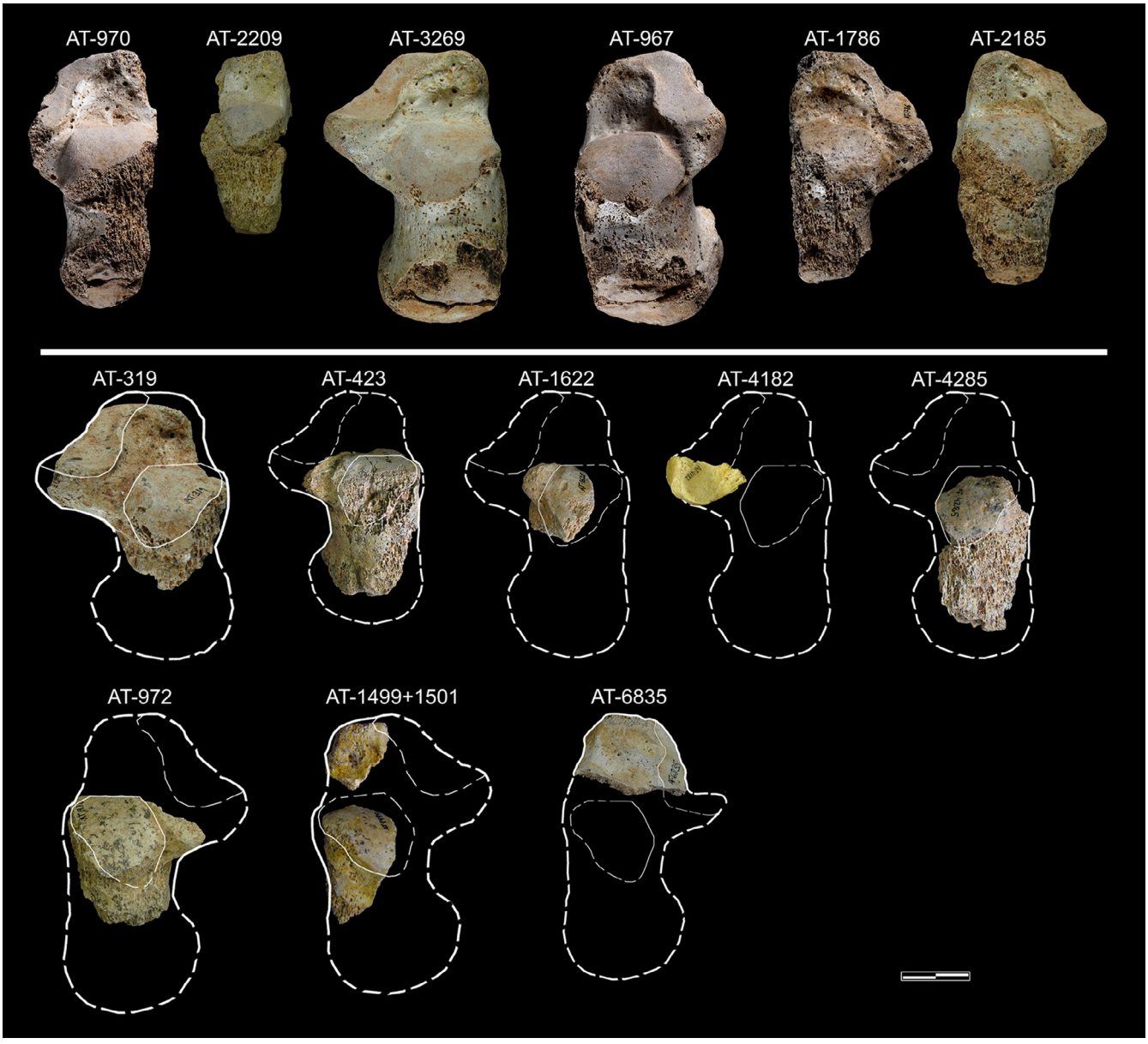

FIGURE 5 Representation of some of the immature calcanei from Sima de los Huesos including nearly complete bones (upper row) and fragments (lower rows) in dorsal view. Scale bar = 2 cm. See Table 7 for details about the identification.

TABLE 7 Inventory of calcanei from SH.

Label	Side	Age	Anatomical description
AT-319	R	Ad	Fragment of calcaneus, with the talar facets and part of upper area of the cuboid articulation.
AT-423	R	Im	Fragment of posterior talar facet and a small portion of the tubercle.
AT-489	R	Ad	Complete.
AT-663	L	Ad	Complete.
AT-705	R	Im	Fragment of epiphysis of the posterior tubercle (not figured).
AT-967	L	Ado	Complete. Posterior tubercle partially fused.
AT-969	R	Ad	Complete.
AT-970	R	Ado	Nearly complete. Posterior tubercle partially fused.
AT-971	L	Ad	Complete.
AT-972	L	Ad?	Fragment of posterior talar facet.
AT-981	R	Ad	Complete
AT-1499[a]	L	Im	Fragment of posterior talar facet.
AT-1501[a]	L	Im	Fragment of cuboid facet.
AT-1576	R	Ad	Nearly complete
AT-1622	R	Im?	Fragment of posterior talar facet and a small part of sulcus calcaneus.
AT-1645	-	Im	Fragment of epiphysis of the posterior tubercle (not figured).
AT-1740	L	Ad	Complete.
AT-1786	L	Im	Complete.
AT-2185	L	Im	Complete.
AT-2209	R	Im	Complete.
AT-2466	R	Ad	Complete.
AT-2741	R	Ad	Complete.
AT-3130	R	Ad	Complete.
AT-3131	L	Ad	Complete.
AT-3269	R	Ado	Complete. The posterior tubercle is partially fused.
AT-3771	L	Ad	Complete.
AT-4182	R	Ad?	Fragment of *sustentaculum tali*.
AT-4285	R	Im	Highly eroded fragment of posterior talar facet.
AT-4426	L	Ad	Complete with a strong insertion for the Achilles tendon.
AT-6835	L	Ad?	Fragment of anterior-medial talar and cuboid facets.

Note: Ad = Adult (>17 years old), Ado = Adolescent (calcaneal tuber partially fused; 11–17 years old), Im = Immature (<11 years old), according to Cardoso and Severino (2010). R = Right, L = Left.
Abbreviation: SH, Sima de los Huesos.
[a]AT-1499 and AT-1501 are parts of the same calcaneus.

expanded with projected sustentaculum tali when compared to recent *H. sapiens* (Gómez-Olivencia et al., 2020; Pablos et al., 2019; Trinkaus, 1975, 1983b; Trinkaus, 2016).

In SH paleodeme, the calcanei are as broad as Neandertals with long posterior calcaneal tubercles (Table 2). Albeit in this last character, SH calcanei are not significantly longer

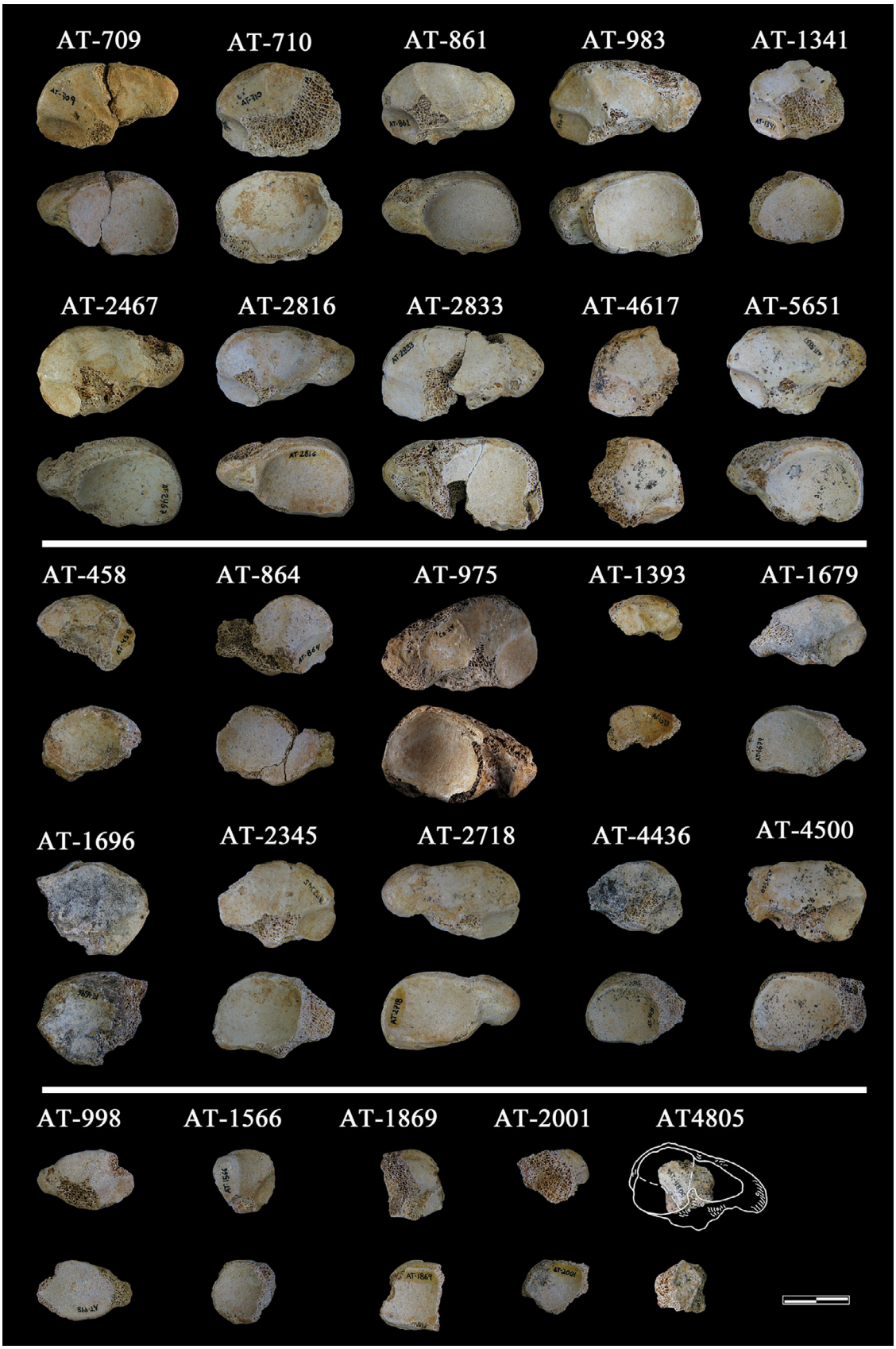

FIGURE 6 Representation of some of the naviculars from Sima de los Huesos including right adult complete or nearly complete bones (upper rows), left adult complete or nearly complete bones (intermediate rows) and immature ones (lower row) in distal and proximal views. Scale bar = 2 cm. See Table 8 for details about the identification.

than the UP group. The calcaneus from SH displays larger tubercles on average in absolute terms than those from the Upper Paleolithic populations. One of the metric traits differentiating SH from Neandertals is the even more projected sustentaculum tali in SH (Pablos et al., 2014). When we compared the sustentacular index [M6 × 100/(M2 − M6)] with the other comparative samples, SH calcanei showed significant differences ($p < 0.05$) with all the groups.

3.3 | Navicular

The navicular human sample recovered in the SH site amounts to 25 elements (Figure 6). All of them correspond to 15 individuals according to the most repeated element; 10 right adult specimens and 5 immature ones differ in measurements and proportions (Pablos et al., 2017). Of the adult individuals, three have been classified as males and three as females (Table 1). Most of the naviculars from SH are complete or nearly complete. For a description of these fossils, see Table 8.

It was previously established that Neandertal navicular is wide, both absolutely and relatively in relation to the dorsoplantar height when compared to both recent and fossil *H. sapiens* (Harvati et al., 2013; Pablos et al., 2018; Pomeroy et al., 2017; Sala et al., 2013; Trinkaus, 1983b). The navicular bones from SH are similar to Neandertals in the absolute and relative breadth (Figure 2e and Table 3). Although not significantly, the Middle Pleistocene specimen from Jinniushan 1 is narrower than the average of Neandertals and SH naviculars (Lu et al., 2011).

3.4 | Cuboid

In the SH site, 23 cuboid bones have been recovered (Figures 7 and 8), which represents one more from the last inventory (Pablos et al., 2017). The minimum

TABLE 8 Inventory of naviculars from SH.

Label	Side	Age	Anatomical description
AT-458	L	Ad	Complete. Eroded at the tuberosity.
AT-709	R	Ad	Complete (two fragments).
AT-710	R	Ad	Complete. Eroded at the tuberosity.
AT-861	R	Ad	Complete.
AT-864	L	Ad	Complete. Eroded at the tuberosity.
AT-975	L	Ad	Complete.
AT-983	R	Ad	Complete.
AT-998	L	Im	Complete. Eroded.
AT-1341	R	Ad	Eroded at the tuberosity and distal area.
AT-1393	L	Ad	Dorsal fragment.
AT-1566	L	Im	Fragment eroded at plantar and medial zones.
AT-1679	L	Ad	Complete. Eroded at the tuberosity.
AT-1696	L	Ad	Nearly complete. Eroded at the tuberosity.
AT-1869	L	Im	Fragment eroded at the medial and lateral sides.
AT-2001	L	Im	Fragment eroded.
AT-2345	L	Ad	Nearly complete. Eroded at the tuberosity.
AT-2467	R	Ad	Complete.
AT-2718	L	Ad	Complete.
AT-2816	R	Im	Complete.
AT-2833	R	Ad	Complete. Eroded at the plantar area.
AT-4436	L	Ad?	Nearly complete. Eroded at the tuberosity.
AT-4500	L	Ad	Nearly complete. Eroded at the tuberosity.
AT-4617	R	Ad	Lateral fragment eroded.
AT-4805	R	Inm	Small fragment eroded.
AT-5651	R	Ad	Complete.

Note: L = left. R = Right. Ad = Adult. Im = Immature.
Abbreviation: SH, Sima de los Huesos.

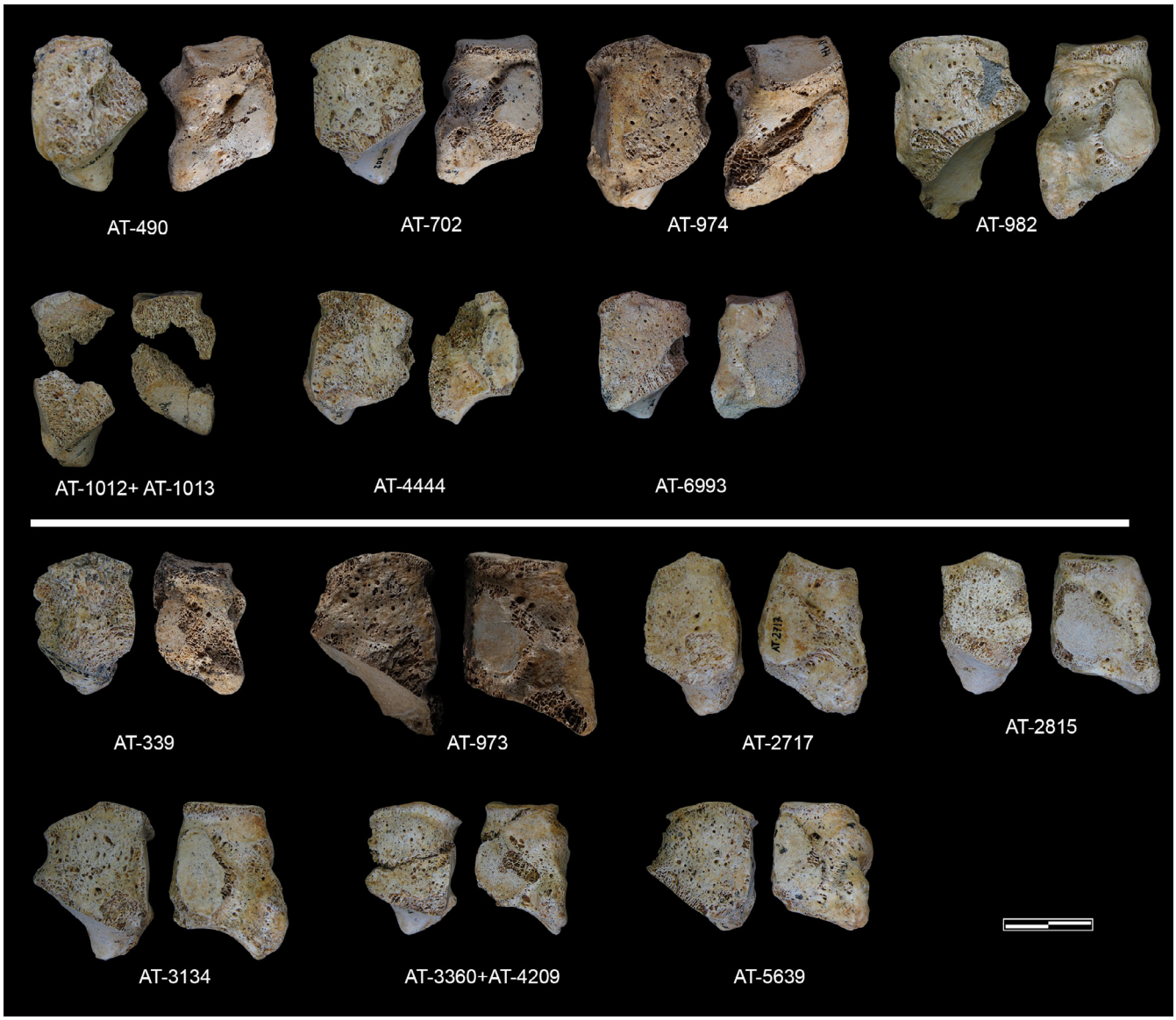

FIGURE 7 Representation of some of the cuboids from Sima de los Huesos including right bones (upper rows) and left ones (bottom rows) in dorsal and medial view. Note that AT-1012 + AT-1013 is displayed in dorsal and lateral views. Scale bar = 2 cm. See Table 9 for details about the identification.

number of elements and individuals is 18 and 10, respectively. Seven of the cuboids correspond to adult elements and three are immature ones. We can establish that three of the adults probably belonged to male individuals, and one likely is from a female (Table 1). The anatomical description of the cuboid sample from SH is offered in Table 9.

Prior to Neandertals and *H. sapiens*, a few *Homo* cuboid bones have been recovered in the human fossil record, and most of them belonged to small-sized species that make direct comparisons difficult, because it is unknown exactly when the modern morphology of the cuboid arose and its morphological relationship with Neandertals. The Neandertal cuboids are robust and anteroposteriorly short (Trinkaus, 1975). The cuboids from SH are significantly anteroposteriorly shorter than those of UP and recent *H. sapiens* (Figure 2). However, the Middle Paleolithic modern human specimens Qafzeh 9 and Skhul 4 are as short as the cuboids of Neandertals and SH. Thus, establishing an evolutionary polarity in this trait is highly speculative until more cuboids belonging to the genus *Homo* are discovered. Although not significantly different, both Neandertals and SH cuboids are proximally narrower than the average of the recent and fossil *H. sapiens*. In this trait, the Middle Pleistocene cuboid from Jinniushan (Lu et al., 2011) is narrower than all the comparative samples.

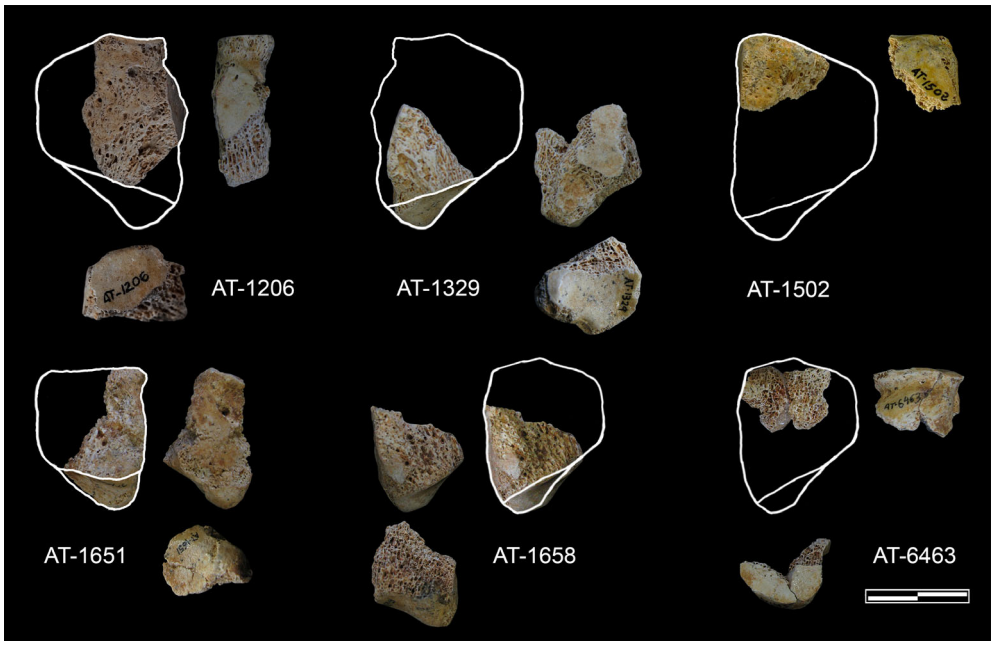

FIGURE 8 Representation of some of the fragmentary cuboids from Sima de los Huesos in several views. Scale bar = 2 cm. See Table 9 for details about the identification. Note that AT-6463 is displayed in dorsal, plantar, and distal views.

TABLE 9 Inventory of cuboids from SH.

Label	Side	Age	Anatomical description
AT-339	L	Ad	Complete. Eroded.
AT-490	R	Ad	Complete.
AT-702	R	Ad	Complete.
AT-973	L	Ad	Complete.
AT-974	R	Ad	Complete.
AT-982	R	Ad	Complete.
AT-1012 + AT-1013	R	Ad	Nearly complete. Two fragments.
AT-1206	L	Ad	Dorsal fragment.
AT-1329	R	Ad	Posterior fragment.
AT-1502	L	Im?	Distal fragment.
AT-1651	L	Im	Medial fragment.
AT-1658	R	Ad?	Posterior fragment.
AT-2717	L	Ad	Complete.
AT-2815	L	Im	Complete. Slightly eroded.
AT-3134	L	Ad	Complete.
AT-3360 + 4209	L	Ad	Complete. Two fragments.
AT-4444	R	Ad	Complete. Eroded
AT-5639	L	Ad	Complete.
AT-6463	R	Ad	Distal fragment.
AT-6466	-	-	Fragment of lateral cuneiform facet (not figured).
AT-6993	R	Ad	Complete. Eroded

Note: L = left. R = Right. Ad = Adult. Im = Immature.
Abbreviation: SH, Sima de los Huesos.

3.5 | Medial cuneiform

In the SH paleodeme, 15 medial cuneiforms are represented (Figure 9 and Table 10), which represent at least nine individuals. Six adult individuals are established with the left ones, and the other three are estimated based on three left immature medial cuneiforms. From the adult individuals, we consider three as likely males and one as female (Table 1).

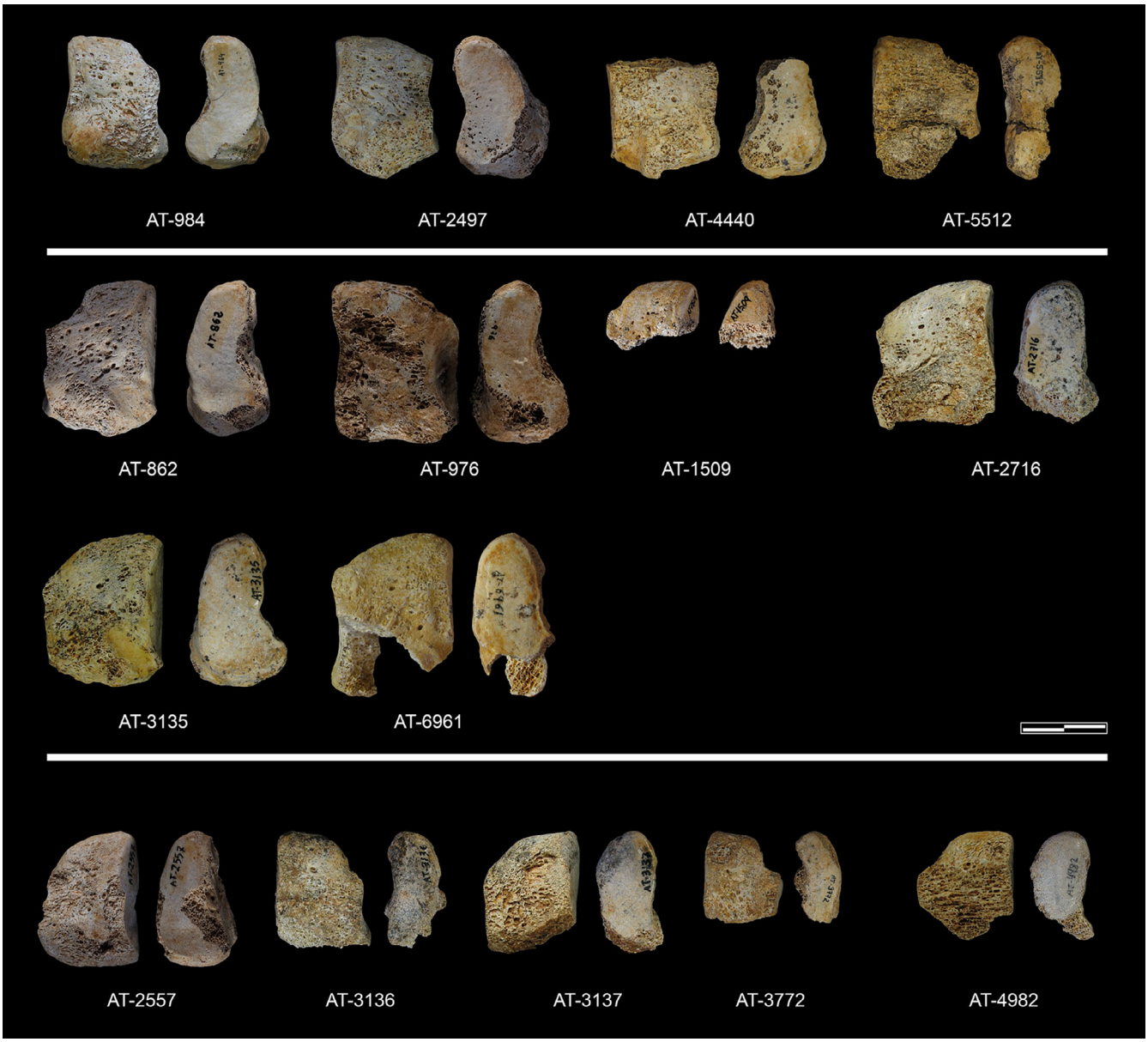

FIGURE 9 Representation of the medial cuneiforms from Sima de los Huesos including complete right adult bones (upper row), complete left adult bones (intermediate rows), and immature medial cuneiforms (lower row) in medial and distal views. Scale bar = 2 cm. See Table 10 for details about the identification.

The metric dimensions of the SH medial cuneiform sample are displayed in Table 3. The antero-posterior length of the different samples does not show significant differences among the comparative samples and SH. Besides those cuboids from SH, Neandertals, and *H. sapiens*, in the *Homo* fossil record, there are three medial cuneiforms with this measurement available; D4110 from Dmanisi (Jashashvili et al., 2010), OH8 from Olduvai (Day & Napier, 1964) and UW 101–1535 from Dinaledi Chamber (Harcourt-Smith et al., 2015). These last three are shorter than all the comparative samples. These three medial cuneiforms belonged to small-sized species inside genus *Homo*, and probably that is the reason for the short length instead of any other phylogenetic establishment. However, the basal breadth of the medial cuneiform (Table 3 and Figure 10a) is significantly larger in SH than in recent populations. Neandertals do not display significant differences with recent and fossil *H. sapiens*. The specimen of Tianyuan (Shang & Trinkaus, 2010) displays a narrow medial cuneiform like those of recent and fossil *H. sapiens*. All of this suggests that a broad medial cuneiform could represent

an exclusive trait of the SH population different from Neandertals and *H. sapiens*. More medial cuneiforms from Early and Middle Pleistocene fossils are needed in order to confirm or refute this statement.

TABLE 10 Inventory of medial cuneiforms from SH.

Label	Side	Age	Anatomical description
AT-862	L	Ad	Complete.
AT-976	L	Ad	Complete.
AT-984	R	Ad	Complete.
AT-1509	L	Ad	Dorsal fragment.
AT-2497	R	Ad	Complete.
AT-2557	L	Im	Complete.
AT-2716	L	Ad	Complete.
AT-3135	L	Ad	Complete.
AT-3136	R	Im	Complete. Eroded.
AT-3137	L	Im	Complete. Eroded.
AT-3772	R	Im	Complete. Eroded.
AT-4440	R	Ad	Plantar fragment.
AT-4982	L	Im	Dorsal fragment
AT-5512	R	Ad	Nearly complete. Eroded
AT-6961	L	Ad	Nearly complete. Eroded

Note: L = left. R = Right. Ad = Adult. Im = Immature.
Abbreviation: SH, Sima de los Huesos.

3.6 | Intermediate cuneiform

Among the SH foot collection, 16 intermediate cuneiforms have been recovered (Figure 11 and Table 11). From them, we identified a minimum of 10 individuals: 8 adults and 2 immatures (Table 1).

When we compared the dorsal length of the intermediate cuneiform, we see that those from SH are significantly shorter than those of Neandertals, UP, and recent *H. sapiens* (Figure 10). Apart from the small-sized individuals from Dinaledi Chamber (Harcourt-Smith et al., 2015), there are no other large-sized *Homo* specimens with which to compare. Interestingly, there are four MPMH individuals that preserve the intermediate cuneiform, and they are as short as those from SH. The small sample size of this group precludes any firm conclusion about the evolutionary polarity of this character. Anyway, the short intermediate cuneiform from SH is different from their descendants the Neandertals in this trait, which allows differentiation among these two populations.

3.7 | Lateral cuneiform

In the SH site, 14 lateral cuneiforms have been recovered and identified (Figure 12 and Table 12). The sample of lateral cuneiforms is represented by at least eight

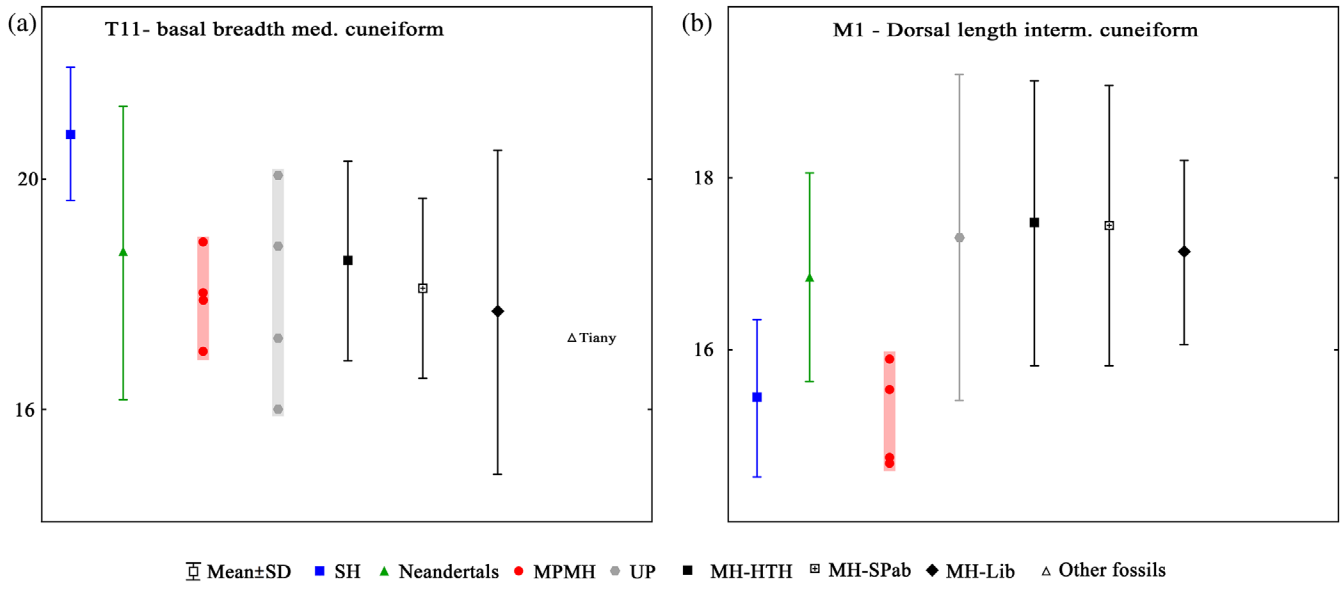

FIGURE 10 Univariate analysis of the Sima de los Huesos (SH) cuneiforms remains. MH-HTH, Modern humans-Hamann-Todd Osteological collection; MH-Lib, Modern Humans-Libben-Amerindians collection (unshod); MH-SPab, San Pablo Medieval collection; MPMH, Middle Paleolithic modern humans; SD, standard deviation; UP, Upper Paleolithic. (a) Plantar breadth of medial cuneiform (in mm). (b) Superior length (M1) of the intermediate cuneiform (in mm). Tiany, Tianyuan.

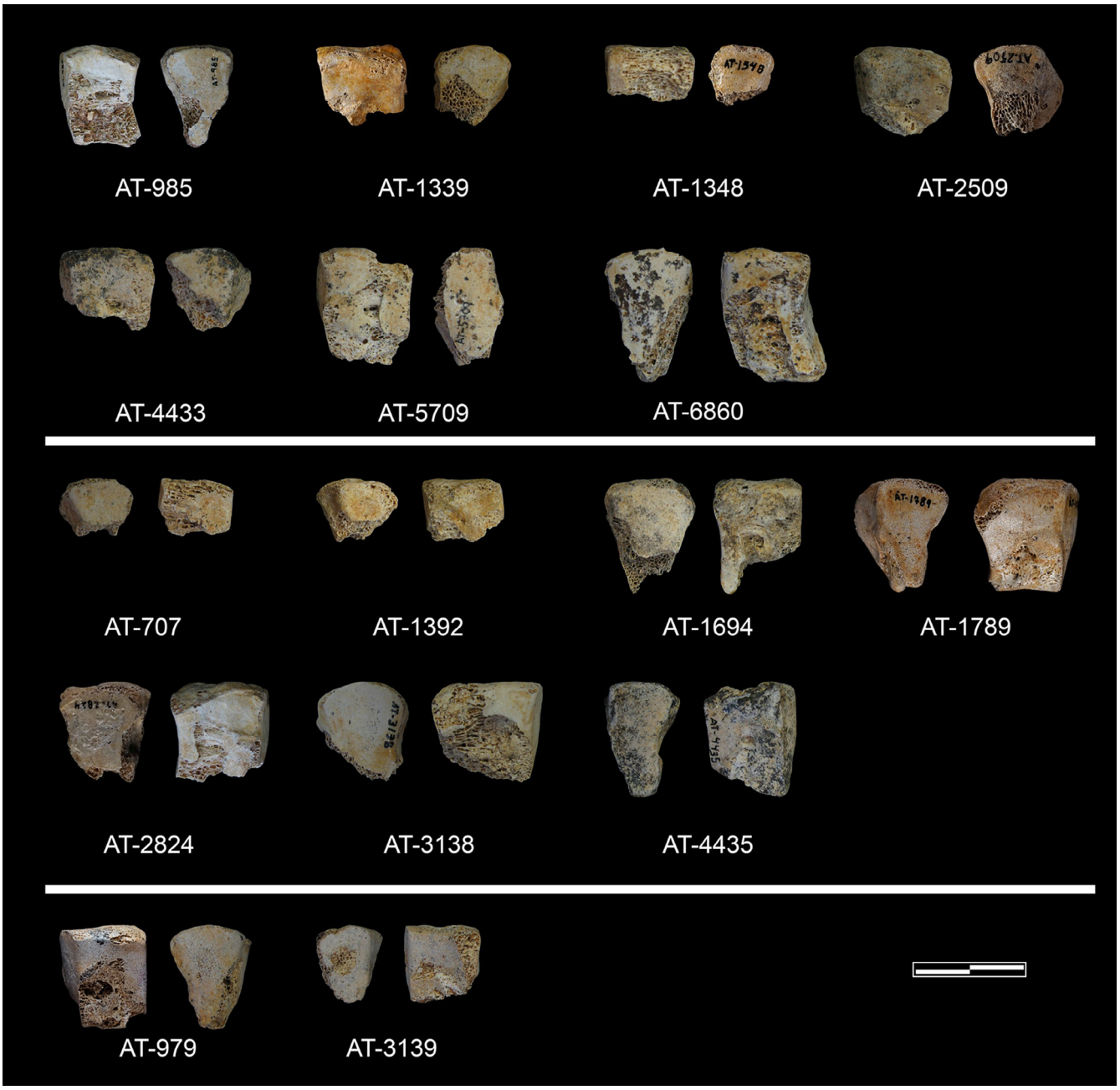

FIGURE 11 Representation of some of the intermediate cuneiforms from Sima de los Huesos in lateral view. Scale bar = 2 cm. See Table 11 for details about the identification.

individuals: six adult ones and two immatures. Among the adult individuals, we estimate one as belonging to a male and the other to a female.

When we compare the length of the lateral cuneiform in the different comparative samples with SH (Table 3), we see that those of Neandertals are shorter on average than both those of recent and fossil *H. sapiens*, but not in a significant way. The lateral cuneiforms from SH are significantly shorter than the lateral cuneiforms of recent and fossil *H. sapiens*,

4 | MAIN ANATOMICAL TRAITS

The tarsals from the SH site are generally more robust than the comparative samples (Table 13). In some ways, this robusticity pattern is similar to that observed in Neandertals, as is the case with the broad tali, calcanei, and naviculars. This is in accordance with the general robusticity of other elements of the postcranial skeleton (Arsuaga et al., 2015; Bonmatí et al., 2010; Carretero, García-González, et al., 2024; Carretero, Rodríguez,

TABLE 11 Inventory of intermediate cuneiforms from SH.

Label	Side	Age	Anatomical description
AT-707	L	Ad?	Dorsal fragment.
AT-979	R	Im	Complete.
AT-985	R	Ad	Complete.
AT-1339	R	Ad	Dorsal fragment.
AT-1348	R	Ad	Dorsal fragment.
AT-1392	L	Ad	Dorsal fragment.
AT-1694	L	Ad	Nearly complete.
AT-1789	L	Ad	Complete.
AT-2509	R	Ad	Dorsal fragment.
AT-2824	L	Ad	Dorsal fragment.
AT-3138	L	Ad	Dorsal fragment.
AT-3139	R	Im	Dorsal fragment.
AT-4433	R	Ad	Dorsal fragment.
AT-4435	L	Ad	Complete.
AT-5709	R	Ad	Complete. Eroded.
AT-6860	R	Ad	Complete.

Note: L = left. R = Right. Ad = Adult. Im = Immature.
Abbreviation: SH, Sima de los Huesos.

et al., 2024; García-González et al., 2024; Gómez-Olivencia et al., 2007; Gómez-Olivencia & Arsuaga, 2024; Pablos & Arsuaga, 2024; Rodríguez et al., 2024a, 2024b).

Nevertheless, there are other traits observed in SH tarsal remains that allow us to differentiate from those of Neandertals. The SH tali are even broader than those of the already broad Neandertals and display an absolutely and relatively narrow head. The calcanei of Neandertals show projected sustentaculum tali. In SH, the sustentaculum tali is even more projected than that in Neandertals. Finally, a broad medial cuneiform and a short intermediate cuneiform are different from those of Neandertals. Although these are just a few characters, in some ways, the SH tarsals are even more robust than Neandertals (Table 13). Something similar is observed in metatarsals and phalanges, especially in the hallucal elements (Pablos & Arsuaga, 2024).

Paleobiological inferences (stature and body mass)

Table 14 provides the results of the stature estimates calculated from the talus and calcaneus. These results are similar, albeit slightly higher, to those obtained using the femora and the tibiae from SH: 168.1 ± 3.2 cm ($n = 8$)

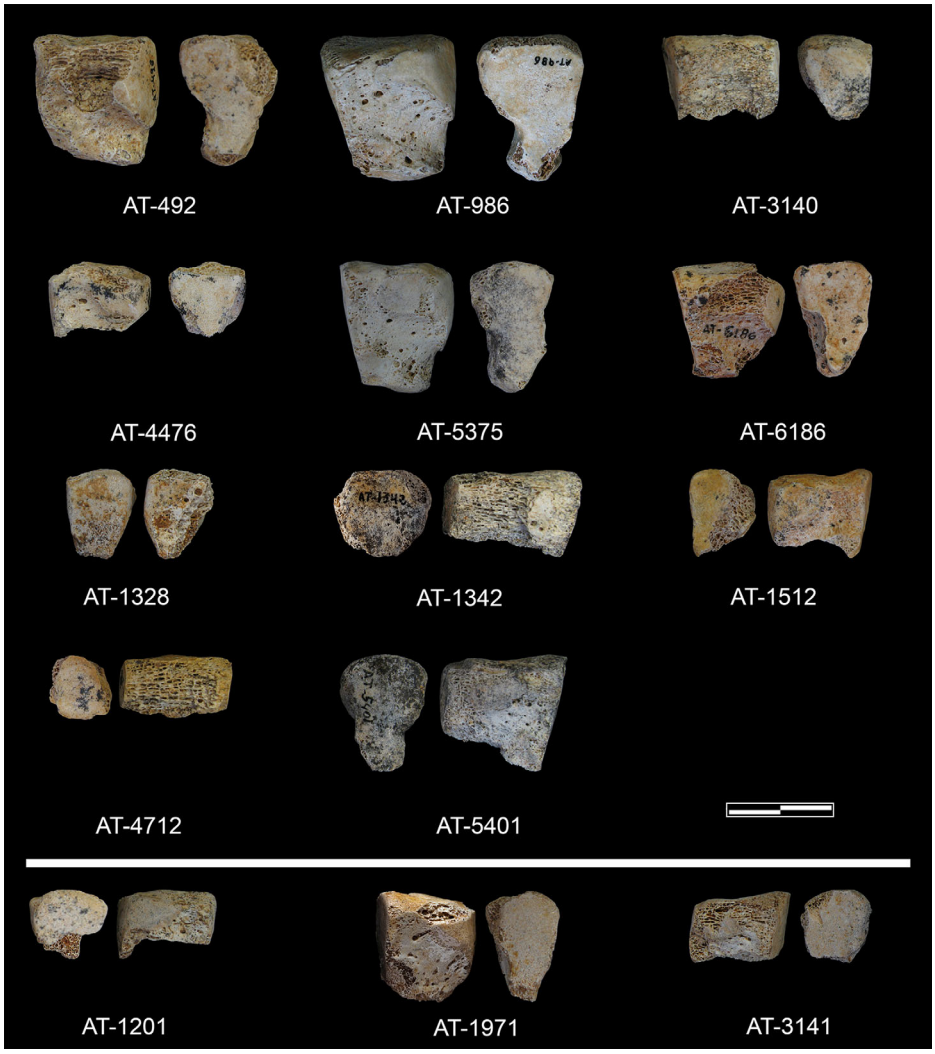

FIGURE 12 Representation of some of the lateral cuneiforms from Sima de los Huesos in lateral view. Scale bar = 2 cm. See Table 12 for details about the identification.

for males, 156.1 ± 2.5 cm ($n = 2$) for females, and 165.7 ± 5.8 cm ($n = 10$) for the entire SH sample of femora and tibiae (Carretero et al., 2012).

In Table 14, we provide the average body mass estimates for males, females, and the total sample altogether.

Considering the body mass estimates of the foot associations (foot 1 and foot 2), and keeping in mind that the tarsals (89.2–92.2 kg) and metatarsals estimates are similar to the results from pelvis 1 (Pablos et al., 2017; Pablos & Arsuaga, 2024), we suggest here that these feet could belong to the same large individual as pelvis 1 from the SH collection, or at least to one similar in proportions and body size.

The estimated body mass average for the human tali sample from SH is 69.7 ± 10.0 kg, and the mean estimated stature calculated with the talus is 173.9 ± 1.4 cm for males and 161.9 ± 2.3 cm for females (Table 14). In spite of that, the estimate based on the bi-iliac breadth of Pelvis 1 from SH (90.3–92.5; Bonmatí et al., 2010) is well above the mean of the estimates based on the talus from SH (more than two standard deviations). There are also two associated tali from the same individual (AT-965 and AT-2495; Pablos, Martínez, et al., 2013), whose estimates are basically indistinguishable (89.2–92.2).

TABLE 12 Inventory of lateral cuneiforms from SH.

Label	Side	Age	Anatomical description
AT-492	R	Ad	Complete.
AT-986	R	Ad	Complete.
AT-1201	L	Im?	Dorsal fragment.
AT-1328	L	Ad	Dorsal fragment.
AT-1342	L	Ad	Dorsal fragment.
AT-1512	L	Ad	Dorsal fragment.
AT-1971	R	Im	Complete. Eroded.
AT-3140	R	Ad	Dorsal fragment.
AT-3141	L	Im	Dorsal fragment.
AT-4476	R	Ad	Dorsal fragment.
AT-4712	L	Ad	Dorsal fragment.
AT-5375	R	Ad	Complete.
AT-5401	L	Ad	Complete.
AT-6186	R	Ad	Complete. Eroded

Note: L = left. R = Right. Ad = Adult. Im = Immature.
Abbreviation: SH, Sima de los Huesos.

5 | TARSAL ASSOCIATIONS

We cautiously propose here the most likely associations among different tarsals at this point, taking into account the current state of the foot collection into SH. These associations are based on the general size, metric dimensions, shape, general morphology, and that of the articular facets, bilateral asymmetry, state of development, anatomical congruence, and so on. The previously

TABLE 13 Summary of selected traits in tarsals in fossil and extant humans.

Element	Trait	*H. ergaster/erectus*	*H. antecessor*	SH	Neandertals	*H. sapiens*
Talus	Lateral malleolar fact	Variable	-	+ Broad	Broad	Narrow
	Head	Absolutely and relatively arrow	Absolutely broad and relatively narrow	Absolutely and relatively Narrow	Absolutely and relatively Broad	Intermediate
	Neck	Short	Short	Short	Short	Long
Calcaneus	General breadth	-	-	Broad	Broad	Narrow
	Sustentaculum tali	-	-	Well projected	Projected	Less projected
Navicular	General size	Narrow?	-	Broad	Broad	Narrow
Cuboid	General size	-	-	Short	Short	Long
Medial cuneiform	General size	-	-	Broad	Narrow	Narrow
Intermediate cuneiform	General size	-	-	Short	Long	Long and short (?)
Distal cuneiform	General size	-	-	Short	Short (?)	Long

Note: Plesiomorphic (red) and derived or autapomorphic (blue) trait for Sima de los Huesos (SH), *H. neanderthalensis*, and *H. sapiens* clades. Traits exclusive to SH relative to Neandertals are shown in green. Colorless cells indicate uncertain polarity. *H. sapiens* clade includes both recent and fossil samples. Modified and updated from Arsuaga et al. (2015).

established sex assignment also provides us with additional information to be used in the association of different elements.

5.1 | Foot 1 and foot 2 association

From different field campaigns, several tarsals and metatarsals were recovered from the SH site, which likely belonged to two nearly complete feet of the same male adult individual. They correspond to the named foot 1 (right) and foot 2 (left) from the SH foot collection (Pablos et al., 2015). This association was done based on their state of development, general size, anatomical congruence, bilateral asymmetry, and sexual assignment (Figure 13).

The complete set of tarsometatarsal associations preserves almost all of the tarsals from both sides, except for the left lateral cuneiform. Both tali and calcanei have been identified as male within the SH foot variation (Pablos et al., 2014, 2017; Pablos, Martínez, et al., 2013). This male individual is one of the largest in the SH foot collection. All the epiphyses are completely fused, and the general stage of development indicates that they belong to an adult individual. All of the elements associated with foot 1 and foot 2 fit correctly in pairs: for example, the right talus articulates perfectly with the right calcaneus, which also fits with the cuboid, and so on. This is also the case for all articulation among tarsals and metatarsals (Pablos & Arsuaga, 2024).

The average stature calculated from the tali and calcanei from both sides is 174.5 ± 1.4 cm for this foot association. Using the formula of least squares for human-based regression provided by McHenry and Berger (1998) for the tali from foot 1 and foot 2, we obtained an average body mass for this individual of 90.7 ± 2.1 kg. These estimates are similar to those of pelvis 1 from SH, one of the biggest in the SH collection (Bonmatí et al., 2010). The body mass index for the tarso-metatarsal skeleton of foot 1 and foot 2 calculated here as the body mass (in kg) divided by height squared (in m) is 27.74 which could suggest that some individuals were overweight, according to the International Obesity Task Force (Cole & Lobstein, 2012). This fact suggests that the musculature of this individual, and that from all the individuals from SH, is higher than that observed in recent modern humans because the corporal thoracic cylinder is broader than in recent populations (Arsuaga et al., 1999;

TABLE 14 Stature (in cm) and body mass (in kg) estimates from the SH tarsals.

	Talus	Calcaneus
	Stature from tarsals	
Male	173.9 ± 1.4 ($n = 6$)	175.7 ± 1.9 ($n = 7$)
Female	161.9 ± 2.3 ($n = 7$)	160.6 ± 1.4 ($n = 3$)
All	167.4 ± 6.0 ($n = 15$)	179.9 ± 6.9 ($n = 13$)
	Body mass from Tali	
Male	78.9 ± 10.3 ($n = 6$)	-
Female	64.6 ± 7.0 ($n = 8$)	-
All	69.7 ± 10.0 ($n = 20$)	-

Note: Mean ± standard deviation and sample size (n) are shown.
Abbreviation: SH, Sima de los Huesos.

FIGURE 13 Representation of the foot 1 and foot 2 associations proposed inside the SH foot collection. SH, Sima de los Huesos.

Carretero et al., 2018; Carretero, Rodríguez, et al., 2024; García-González et al., 2024; Gómez-Olivencia et al., 2010; Rodríguez et al., 2018, 2016, 2024b).

This individual denotes the high robusticity of the SH Middle Pleistocene population, that is, for the same stature, the bodies are broader than those of modern and fossil *H. sapiens*. The bauplan of "wide *Homo*" with a large thorax, broad shoulders and pelves likely comes from earlier species/populations such as *Homo ergaster/antecessor*, from which *H. sapiens* departed (Arsuaga, 2010; Arsuaga et al., 1999, 2015; Bonmatí et al., 2010; Carretero et al., 2004; Carretero, Rodríguez, et al., 2024; García-González et al., 2009; Lorenzo et al., 2015; Pablos et al., 2012).

6 | DISCUSSION AND CONCLUSIONS

The talus sample from the SH site generally shows a posteriorly broad trochlea, a very broad lateral malleolar facet, a short neck, and a narrow head. The neck of the talus is short in all the *Homo* fossils except those of *H. sapiens*, probably due to the inverse relationship between the trochlea length and the neck (Rhoads & Trinkaus, 1977). A broad lateral malleolar facet could represent a primitive or plesiomorphic trait inherited from an African ancestor. Nevertheless, in other Early and Middle Pleistocene tali (KNM-ER 1476a, KNM-ER 5428, and OH 8), this facet is significantly narrower than those of SH and Neandertals, demonstrating the difficulty of establishing the primitive/plesiomorphic or derivate/autapomorphic condition of this trait. Usually, the talar trochlea is described as wedge-shaped in recent *H. sapiens*, but this morphology is not related to the movement of the fibula nor to the plantarflexion of the ankle (Barnett & Napier, 1953). In SH and Neandertals, the trochlea is more rectangular than in *H. sapiens*. This similarity between SH and Neandertals likely reflects the evolutionary relationship between these two populations rather than biomechanical factors.

The Neandertal calcanei show long and robust bodies for the insertion of the triceps surae muscle group, which is related to the absorption of the stress of the heel during the stance phase of the gait (Raichlen et al., 2011; Trinkaus, 1983a). The posterior calcaneal tubercle is long in Neandertals relative to anatomically modern humans (Raichlen et al., 2011). The calcaneus bones from the SH site are broad with relatively and absolutely broad sustentaculum tali, which could represent an exclusive trait of this Middle Pleistocene population. These broad and robust calcanei from Neandertals, and especially from SH, could support the evolutionary relationship previously established between these two populations or the fact that both populations display a large body size (Arsuaga et al., 1999; Bonmatí et al., 2010; García-González et al., 2024). Nevertheless, the highly broad sustentaculum tali observed in SH calcanei suggests that the SH population is more robust than their descendants, the Neandertals, at least in this trait and the lateral malleolar facet of the talus (see above). The combination of these traits allows us to differentiate between the SH calcanei and those of Neandertals and *H. sapiens*.

There are not many more naviculars in the *Homo* fossil record, apart from those from the small-sized species such as *Homo floresiensis*, *H. naledi*, and the OH8 specimen (Day & Napier, 1965; Harcourt-Smith et al., 2015; Jungers et al., 2009), which makes difficult to establish evolutionary relationships for this bone in human evolution. However, the current data suggest that a broad navicular represents a Neandertal-derived or autapomorphic trait shared by the Neandertals and their ancestors, the hominins from SH.

The absolutely and relatively broad SH and Neandertal naviculars are likely related to the robusticity of these populations. This pattern also confirms the evolutionary relationship among these Pleistocene populations. The primitive or plesiomorphic condition is likely that which is observed in *H. sapiens*, and a broad navicular could represent a derived or autapomorphic trait in the SH-Neandertal lineage.

The proximally narrower cuboids of Neandertals and SH hominins, and the narrower one of the Jinniushan individual (Lu et al., 2011), suggest that a narrow cuboid could be a primitive or plesiomorphic character within the genus *Homo*. The lateral cuneiform of Neandertals and those of the SH population are shorter than those of recent and fossil *H. sapiens*. This could be identified as a shared trait in the evolutionary line of Neandertals. Again, more foot fossils are needed to clearly establish the polarity of this character.

With these data on mind, the evolutionary relationship among SH and Neandertals is confirmed based on the morphology of the foot.

The studies of the postcranial skeleton of the SH hominins have allowed to establish some traits similar among this Middle Pleistocene population and Neandertals (Arsuaga et al., 2015; Carretero et al., 1997; García-González et al., 2024; Gómez-Olivencia & Arsuaga, 2024; Pablos et al., 2017; Rodríguez et al., 2024a). The study of tarsals carried out here also found similar traits in SH relative to Neandertals that differentiate both populations from recent *H. sapiens*. This confirms the evolutionary relationship between these two paleodemes as evolutionary sister groups as previously established by other anatomical regions (Arsuaga et al., 2014, 2015;

Carretero, García-González, et al., 2024; Pablos, Martínez, et al., 2013; Rodríguez et al., 2024a). This similarity in postcranial anatomical traits between SH and Neandertals is likely related to a high degree of biomechanical stress, and to the greater general robustness of the postcranial skeleton. However, in some traits, the forefoot from the SH collection exhibits subtle differences with Neandertals, such as a very broad lateral malleolar facet and a narrow head in the talus, a well-projecting sustentaculum tali of the calcaneus, a broad medial cuneiform, and a short intermediate cuneiform (Table 13).

The near absence of tarsals of other *Homo* species tentatively precludes us from ascertaining more in-depth evolutionary relationships with other *Homo* species. But this robusticity pattern probably constitutes the primitive-plesiomorphic condition inherited from *H. antecessor* or other earlier species of genus *Homo* (Arsuaga, 2010; Lorenzo et al., 2015; Lu et al., 2011; Pablos et al., 2012), or it could represent shared traits by the SH-Neandertals evolutionary line (Arsuaga et al., 2014, 2015; Arsuaga, Martínez, Gracia, & Lorenzo, 1997; García-González et al., 2024; Pablos et al., 2014; Pablos, Martínez, et al., 2013).

In some elements, we observed that the SH tarsals are even more robust than in Neandertals (see above). These traits observed in the tarsals are the projected lateral malleolar facet of the talus (Pablos, Martínez, et al., 2013), the well-projected sustentaculum tali of the calcaneus (Pablos et al., 2014), and the broad medial cuneiform. This is observed in the hallux of SH (Pablos & Arsuaga, 2024), but also in other anatomical elements of the postcranial skeleton. The SH pelvis displays a bi-iliac breadth that is broader than that of Neandertals, the iliac height and the maximum sacral breadth have lower values in Neandertals, and the pubic ramus is craniocaudally thinner in Neandertals relative to the SH sample (Arsuaga et al., 2015; Bonmatí et al., 2010). The humeral cortical area of the SH sample is higher than that of Neandertals (Arsuaga et al., 2015). The posterior arch of the atlas in SH hominins is more robust than the slender ones observed in Neandertals (Arsuaga et al., 2015; Gómez-Olivencia et al., 2007; Gómez-Olivencia & Arsuaga, 2024). The lumbar vertebrae and the transverse process in the third lumbar in SH are larger and longer, respectively, in SH relative to Neandertals (Bonmatí et al., 2010). The SH first ribs have a tuberculo-ventral chord that is larger than in Neandertals (Gómez-Olivencia et al., 2010). The SH radii are longer than in Neandertals, and the neck and diaphysis are mediolaterally larger (Rodríguez et al., 2016). Taking into account the stature estimates, Neandertals probably had slightly reduced stature, albeit not significantly, compared with their ancestors: the people from SH (Arsuaga et al., 2015; Carretero et al., 2012; Will et al., 2017). All of this suggests a slight gracilization process of the foot in the SH-Neandertal lineage. These traits of robusticity in the SH tarsals are proposed here as exclusive traits to this Middle Pleistocene population with respect to Neandertals and the rest of the known genus *Homo*. In the *Homo* fossil record, there is a nearly ubiquitous absence of tarsal remains excluding Neandertals and fossil *H. sapiens*. The fact that in SH, all anatomical elements of the postcranial skeleton have been recovered, including all the posterior and anterior tarsals, suggests that complete skeletons were deposited at the SH chamber (Arsuaga et al., 1990; Sala, Martínez, et al., 2024).

The study of the rearfoot from the SH site has allowed us to establish some likely primitive or plesiomorphic traits in this population. This is likely related to general robusticity of the body in the SH hominins (Arsuaga et al., 2015; Bonmatí et al., 2010; Carretero et al., 2018; Carretero, Rodríguez, et al., 2024; García-González et al., 2024; Gómez-Olivencia et al., 2007; Pablos et al., 2017; Rodríguez et al., 2024a). Furthermore, the primitive or plesiomorphic biotype observed in the few foot fossils belonging to *H. antecessor* and *H. ergaster/erectus* suggest that a robust bauplan could be inherited in SH hominins from these species (Arsuaga, 2010; Carretero et al., 2004). The fact that some of these traits are shared with Neandertals confirms that SH and Neandertals represent evolutionary sister groups (Arsuaga et al., 2014; Arsuaga, Martínez, Gracia, & Lorenzo, 1997).

AUTHOR CONTRIBUTIONS

Adrián Pablos: Conceptualization; investigation; writing – original draft; writing – review and editing; formal analysis. **Juan Luis Arsuaga:** Conceptualization; investigation; funding acquisition; writing – review and editing; project administration.

ACKNOWLEDGMENTS

We would like to acknowledge all of the other members of the Atapuerca excavation and research team, especially those from the Sima de los Huesos team, for their dedication and effort over more than 40 years of excavation and research. Without their hard work, help, effort, and advice, this study would not have been possible. This research was financed by the Spanish projects PGC2018-093925-B-C33, PGC2018-093925-B-C31 (MCI/AEI/FEDER, UE), and PID2021-122355NB-C31 funded by MCIN/AEI/10.13039/501100011033/FEDER, UE. Part of this research has also been funded by the European Research Council (ERC-DEATHREVOL; Grant agreement No. 949330). AP has been financed by a research grant from Junta de Andalucía, Spain (EMERGIA20_00403). Fieldwork at Atapuerca is annually funded by the Junta de Castilla y León and Fundación Atapuerca. The availability of the comparative

collection, both modern and fossil, would not have been possible without the help and collaboration of multiple institutions and the people who allowed us access to important collections under their care and who kindly provided assistance. We would especially like to thank Y. Haile-Selassie and L. Jellema of the Cleveland Museum of Natural History (CMNH) for access to the Hamann-Todd Osteological Collection and J. M. Carretero of the University of Burgos (UBU) for access to the San Pablo Medieval collection. E. Trinkaus and C. Lorenzo kindly provided some comparative data. We would like to express our deepest gratitude to the editors of this Anatomical Record volume devoted to the Sima de los Huesos material for kindly inviting us to contribute to this manuscript. Lauren Ames kindly reviewed a previous English version of the manuscript. Most of the photographs of the fossils were taken by J. Trueba from Madrid Scientific Films. Finally, we appreciate the helpful comments and suggestions provided by Associate Editor J. M. Carretero and one anonymous reviewer, which significantly improved the article.

ORCID

Adrián Pablos https://orcid.org/0000-0003-1630-4941

REFERENCES

Alonso-Llamazares, C., & Pablos, A. (2019). Sex estimation from the calcaneus and talus using discriminant function analysis and its possible application in fossil remains. *Archaeological and Anthropological Sciences*, *11*, 4927–4946.

Aranburu, A., Arsuaga, J. L., & Sala, N. (2017). The stratigraphy of the Sima de los Huesos (Atapuerca, Spain) and implications for the origin of the fossil hominin accumulation. *Quaternary International*, *433*, 5–21.

Arsuaga, J. L. (2010). Terrestrial apes and phylogenetic trees. *Proceedings of the National Academy of Sciences of the United States of America*, *107*, 8910–8917.

Arsuaga, J. L., Carretero, J. M., Gracia, A., & Martínez, I. (1990). Taphonomical analysis of the human sample from the Sima de los Huesos Middle Pleistocene site (Atapuerca/Ibeas, Spain). *Human Evolution*, *5*, 505–513.

Arsuaga, J. L., Carretero, J. M., Lorenzo, C., Gómez-Olivencia, A., Pablos, A., Rodríguez, L., García-González, R., Bonmatí, A., Quam, R. M., Pantoja-Pérez, A., Martínez, I., Aranburu, A., Gracia-Téllez, A., Poza-Rey, E., Sala, N., García, N., Alcázar de Velasco, A., Cuenca-Bescós, G., Bermúdez de Castro, J. M., & Carbonell, E. (2015). Postcranial morphology of the middle Pleistocene humans from Sima de los Huesos, Spain. *Proceedings of the National Academy of Sciences of the United States of America*, *112*, 11524–11529.

Arsuaga, J. L., Carretero, J. M., Martínez, I., & Gracia, A. (1991). Cranial remains and long bones from Atapuerca/Ibeas (Spain). *Journal of Human Evolution*, *20*, 191–230.

Arsuaga, J. L., Lorenzo, C., Carretero, J. M., Gracia, A., Martínez, I., García, N., Bermúdez de Castro, J. M., & Carbonell, E. (1999). A complete human pelvis from the Middle Pleistocene of Spain. *Nature*, *399*, 255–258.

Arsuaga, J. L., Martínez, I., Arnold, L. J., Aranburu, A., Gracia-Téllez, A., Sharp, W. D., Quam, R. M., Falguères, C., Pantoja-Pérez, A., Bischoff, J., Poza-Rey, E., Parés, J. M., Carretero, J. M., Demuro, M., Lorenzo, C., Sala, N., Martinón-Torres, M., García, N., Alcázar de Velasco, A., ... Carbonell, E. (2014). Neandertal roots: Cranial and chronological evidence from Sima de los Huesos. *Science*, *344*, 1358–1363.

Arsuaga, J. L., Martínez, I., Gracia, A., Carretero, J. M., Lorenzo, C., García, N., & Ortega, A. I. (1997). Sima de los Huesos (Sierra de Atapuerca, Spain). The site. *Journal of Human Evolution*, *33*, 109–127.

Arsuaga, J. L., Martínez, I., Gracia, A., & Lorenzo, C. (1997). The Sima de los Huesos crania (Sierra de Atapuerca, Spain). A comparative study. *Journal of Human Evolution*, *33*, 219–281.

Auerbach, B. M., & Ruff, C. B. (2004). Human body mass estimation: A comparison of "Morphometric" and "Mechanical" methods. *American Journal of Physical Anthropology*, *125*, 331–342.

Barnett, C. H., & Napier, J. R. (1953). The axis of rotation at the ankle joint in man. Its influence upon the form of the talus and the mobility of the fibula. *Journal of Anatomy*, *86*, 1–9.

Bermúdez de Castro, J. M., Martínez de Pinillos, M., Martín-Francés, L., Modesto-Mata, M., García-Campos, C., Arsuaga, J. L., & Martinón-Torres, M. (2024). Dental remains of the Middle Pleistocene hominins from the Sima de los Huesos site (Sierra de Atapuerca, Spain): Maxillary dentition. *The Anatomical Record*. https://doi.org/10.1002/ar.24841

Bermúdez de Castro, J. M., Martínez, I., Gracia-Téllez, A., Martinón-Torres, M., & Arsuaga, J. L. (2021). The Sima de los Huesos middle Pleistocene hominin site (Burgos, Spain). Estimation of the number of individuals. *The Anatomical Record*, *304*, 1463–1477.

Bidmos, M. A., Adebesin, A. A., Mazengenya, P., Olateju, O. I., & Adegboye, O. (2021). Estimation of sex from metatarsals using discriminant function and logistic regression analyses. *Australian Journal of Forensic Sciences*, *53*, 543–556.

Bidmos, M. A., & Dayal, M. R. (2003). Sex determination from the talus of South African Whites by discriminant function analysis. *The American Journal of Forensic Medicine and Pathology*, *24*, 322–328.

Bonmatí, A., Gómez-Olivencia, A., Arsuaga, J. L., Carretero, J. M., Gracia, A., Martínez, I., Lorenzo, C., Bermúdez de Castro, J. M., & Carbonell, E. (2010). Middle Pleistocene lower back and pelvis from an aged human individual from the Sima de los Huesos site, Spain. *Proceedings of the National Academy of Sciences of the United States of America*, *107*, 18386–18391.

Boyle, E. K., & DeSilva, J. M. (2015). A large *Homo erectus* talus from Koobi Fora, Kenya (KNM-ER 5428), and Pleistocene hominin talar evolution. *PaleoAnthropology*, *2015*, 1–13.

Bräuer, G. (1988). Osteometrie. In R. Martin & R. Knuβman (Eds.), (pp. 160–232). Anthropologie. Handbuch der vergleichenden Biologie des menschen, Fisher.

Cardoso, H. F. V., & Severino, R. S. S. (2010). The chronology of epiphyseal union in the hand and foot from dry bone observations. *International Journal of Osteoarchaeology*, *20*, 737–746.

Carretero, J. M., Arsuaga, J. L., & Lorenzo, C. (1997). Clavicles, scapulae and humeri from the Sima de los Huesos site (Sierra de Atapuerca, Spain). *Journal of Human Evolution*, *33*, 357–408.

Carretero, J. M., Arsuaga, J. L., Martínez, I., Quam, R., Lorenzo, C., Gracia, A., & Ortega, A. I. (2004). Los humanos de la Sima de los Huesos (Sierra de Atapuerca) y la evolución del cuerpo en el género *Homo*. In E. Baquedano & S. Rubio (Eds.), *Miscelánea Homenaje a Emiliano Aguirre* (pp. 120–135). Museo Arqueológico Regional de la Comunidad de Madrid.

Carretero, J. M., García-González, R., Rodríguez, L., & Arsuaga, J. L. (2024). Main anatomical characteristics of the hominin fossil humeri from the Sima de los Huesos Middle Pleistocene site, Sierra de Atapuerca, Burgos, Spain: An update. *The Anatomical Record*. https://doi.org/10.1002/ar.25194

Carretero, J.-M., Rodríguez, L., García-González, R., & Arsuaga, J.-L. (2024). Main morphological characteristics and sexual dimorphism of hominin adult femora from the Sima de los Huesos Middle Pleistocene site (Sierra de Atapuerca, Spain). *The Anatomical Record*. https://doi.org/10.1002/ar.25331

Carretero, J. M., Rodríguez, L., García-González, R., Arsuaga, J. L., Gómez-Olivencia, A., Lorenzo, C., Bonmatí, A., Gracia, A., Martínez, I., & Quam, R. (2012). Stature estimation from complete long bones in the Middle Pleistocene humans from the Sima de los Huesos, Sierra de Atapuerca (Spain). *Journal of Human Evolution*, *62*, 242–255.

Carretero, J.-M., Rodríguez, L., García-González, R., Quam, R.-M., & Arsuaga, J.-L. (2018). Exploring bone volume and skeletal weight in the Middle Pleistocene humans from the Sima de los Huesos site (Sierra de Atapuerca, Spain). *Journal of Anatomy*, *233*, 740–754.

Castejón-Molina, P., & Pablos, A. (2021). Sex estimation by third metatarsals in human fossil and recent populations. *Archaeological and Anthropological Sciences*, *13*, 209.

Cole, T. J., & Lobstein, T. (2012). Extended international (IOTF) body mass index cut-offs for thinness, overweight and obesity. *Pediatric Obesity*, *7*, 284–294.

Day, M. H., & Napier, J. R. (1964). Hominid fossils from Bed I, Olduvai Gorge, Tanganyika: Fossil foot bones. *Nature*, *201*, 969–970.

Day, M. H., & Napier, J. R. (1965). Fossil foot bones. *Current Anthropology*, *6*, 419–420.

Demuro, M., Arnold, L. J., Aranburu, A., Sala, N., & Arsuaga, J.-L. (2019). New bracketing luminescence ages constrain the Sima de los Huesos hominin fossils (Atapuerca, Spain) to MIS 12. *Journal of Human Evolution*, *131*, 76–95.

Di Vincenzo, F., Rodriguez, L., Carretero, J. M., Collina, C., Geraads, D., Piperno, M., & Manzi, G. (2015). The massive fossil humerus from the Oldowan horizon of Gombore I, Melka Kunture (Ethiopia, >1.39 Ma). *Quaternary Science Reviews*, *122*, 207–221.

García-González, R., Carretero, J. M., Rodríguez, L., Gómez-Olivencia, A., Arsuaga, J. L., Bermúdez de Castro, J. M., Carbonell, E., Martínez, I., & Lorenzo, C. (2009). Étude analytique d'une clavicule complète de subadulte d'*Homo antecessor* (site de Gran Dolina, Sierra d'Atapuerca, Burgos, Espagne). *L'Anthropologie*, *113*, 222–232.

García-González, R., Rodríguez, L., Salazar-Fernández, A., Arsuaga, J. L., & Carretero, J.-M. (2024). Updated study of adult and subadult pectoral girdle bones from Sima de los Huesos site (Sierra de Atapuerca, Burgos, Spain). Anatomical and age estimation keys. *The Anatomical Record*. https://doi.org/10.1002/ar.25158

Gómez-Olivencia, A., Arlegi, M., Arceredillo, D., Delson, E., Sanchís, A., Núñez-Lahuerta, C., Fernández-García, M., Villalba, M., Galán, J., Pablos, A., Rodríguez-Hidalgo, A., López-Horgue, M. A., Rodríguez-Almagro, M., Martínez-Pillado, V., Rios-Garaizar, J., & Made, J. V. (2020). The Koskobilo (Olazti, Navarre, Northern Iberian Peninsula) paleontological collection: New insights for the Middle and Late Pleistocene in Western Pyrenees. *Quaternary International*, *566*, 113–140.

Gómez-Olivencia, A., & Arsuaga, J. L. (2024). The Sima de los Huesos cervical spine. *The Anatomical Record*. https://doi.org/10.1002/ar.25224

Gómez-Olivencia, A., Carretero, J. M., Arsuaga, J. L., Rodríguez-García, L., García-González, R., & Martínez, I. (2007). Metric and morphological study of the upper cervical spine from the Sima de los Huesos site (Sierra de Atapuerca, Burgos, Spain). *Journal of Human Evolution*, *53*, 6–25.

Gómez-Olivencia, A., Carretero, J. M., Lorenzo, C., Arsuaga, J. L., Bermúdez de Castro, J. M., & Carbonell, E. (2010). The costal skeleton of *Homo antecessor*: Preliminary results. *Journal of Human Evolution*, *59*, 620–640.

Gualdi-Russo, E. (2007). Sex determination from the talus and calcaneus measurements. *Forensic Science International*, *171*, 151–156.

Harcourt-Smith, W. E. H., Throckmorton, Z., Congdon, K. A., Zipfel, B., Deane, A. S., Drapeau, M. S. M., Churchill, S. E., Berger, L. R., & DeSilva, J. M. (2015). The foot of *Homo naledi*. *Nature Communications*, *6*, 8432.

Harvati, K., Darlas, A., Bailey, S. E., Rein, T. R., El Zaatari, S., Fiorenza, L., Kullmer, O., & Psathi, E. (2013). New Neandertal remains from Mani peninsula, Southern Greece: The Kalamakia Middle Paleolithic cave site. *Journal of Human Evolution*, *64*, 486–499.

Jashashvili, T., Ponce de León, M. S., Lordkipanidze, D., & Zollikofer, C. P. E. (2010). First evidence of a bipartite medial cuneiform in the hominin fossil record: A case report from the Early Pleistocene site of Dmanisi. *Journal of Anatomy*, *216*, 705–716.

Jungers, W. L., Larson, S. G., Harcourt-Smith, W. E. H., Morwood, M. J., Sutikna, T., Awe Due, R., & Djubiantono, T. (2009). Descriptions of the lower limb skeleton of *Homo floresiensis*. *Journal of Human Evolution*, *57*, 538–554.

Lorenzo, C., Carretero, J. M., Arsuaga, J. L., Gracia, A., & Martínez, I. (1998). Intrapopulational body size variation and cranial capacity variation in Middle Pleistocene Humans: The Sima de los Huesos sample (Sierra de Atapuerca, Spain). *American Journal of Physical Anthropology*, *106*, 19–33.

Lorenzo, C., Pablos, A., Carretero, J. M., Huguet, R., Vallverdú, J., Martinón-Torres, M., Arsuaga, J. L., Carbonell, E., & Bermúdez de Castro, J. M. (2015). Early Pleistocene human hand phalanx from the Sima del Elefante (TE) cave site in Sierra de Atapuerca (Spain). *Journal of Human Evolution*, *78*, 114–121.

Lu, Z., Meldrum, D. J., Huang, Y., He, J., & Sarmiento, E. E. (2011). The Jinniushan hominin pedal skeleton from the late Middle Pleistocene of China. *Homo*, *62*, 389–401.

Mahakkanukrauh, P., Praneatpolgrang, S., Ruengdit, S., Singsuwan, P., Duangto, P., & Case, D. T. (2014). Sex estimation from the talus in a Thai population. *Forensic Science International*, *240*, 152.e1–152.e8.

Mann, H. B., & Whitney, D. R. (1947). On a test of whether one of two random variables is stochastically larger than the other. *The Annals of Mathematical Statistics*, *18*, 50–60.

McCown, T. D., & Keith, A. (1939). *The stone age of Mount Carmel*. Clarendon Press.

McHenry, H., & Berger, L. R. (1998). Body proportions in *Australopithecus afarensis* and *A. africanus* and the origin of the genus *Homo*. *Journal of Human Evolution*, *35*, 1–22.

McHenry, H. M. (1992). Body size and proportions in Early Hominids. *American Journal of Physical Anthropology*, *87*, 407–431.

Meyer, M., Arsuaga, J. L., de Filippo, C., Nagel, S., Aximu-Petri, A., Nickel, B., Martínez, I., Gracia, A., Bermúdez de Castro, J. M., Carbonell, E., Viola, B., Kelso, J., Prüfer, K., & Pääbo, S. (2016). Nuclear DNA sequences from the Middle Pleistocene Sima de los Huesos hominins. *Nature*, *531*, 504–507.

Meyer, M., Fu, Q., Aximu-Petri, A., Glocke, I., Nickel, B., Arsuaga, J. L., Martínez, I., Gracia, A., Bermúdez de Castro, J. M., Carbonell, E., & Pääbo, S. (2014). A mitochondrial genome sequence of a hominin from Sima de los Huesos. *Nature*, *505*, 403–406.

Mountrakis, C., Eliopoulos, C., Koilias, C. G., & Manolis, S. K. (2010). Sex determination using metatarsal osteometrics from the Athens collection. *Forensic Science International*, *200*, 178.e1–178.e7.

Pablos, A. (2015). The foot in the *Homo* fossil record. *Mitteilungen der Gesellschaft für Urgeschichte*, *24*, 11–28.

Pablos, A., & Arsuaga, J. L. (2024). Metatarsals and foot phalanges from the Sima de los Huesos Middle Pleistocene site (Atapuerca, Burgos, Spain). *The Anatomical Record*. https://doi.org/10.1002/AR.25412

Pablos, A., Gómez-Olivencia, A., García-Pérez, A., Martínez, I., Lorenzo, C., & Arsuaga, J. L. (2013). From toe to head: Use of robust regression methods in stature estimation based on foot remains. *Forensic Science International*, *226*, 299.e1–299.e7.

Pablos, A., Gómez-Olivencia, A., Maureille, B., Holliday, T. W., Madelaine, S., Trinkaus, E., & Couture-Veschambre, C. (2019). Neandertal foot remains from Regourdou 1 (Montignac-sur-Vézère, Dordogne, France). *Journal of Human Evolution*, *128*, 17–44.

Pablos, A., Lorenzo, C., & Arsuaga, J. L. (2015). Two feet from the same individual from the Middle Pleistocene site of Sima de los Huesos. In R. M. Quam & J. L. Arsuaga (Eds.), *84th Annual Meeting of the American Association of Physical Anthropologists* (p. 245). American Association of Physical Anthropologists (AAPA).

Pablos, A., Lorenzo, C., Martínez, I., Bermúdez de Castro, J. M., Martinón-Torres, M., Carbonell, E., & Arsuaga, J. L. (2012). New foot remains from the Gran Dolina-TD6 Early Pleistocene site (Sierra de Atapuerca, Burgos, Spain). *Journal of Human Evolution*, *63*, 610–623.

Pablos, A., Martínez, I., Lorenzo, C., Gracia, A., Sala, N., & Arsuaga, J. L. (2013). Human talus bones from the Middle Pleistocene site of Sima de los Huesos (Sierra de Atapuerca, Burgos, Spain). *Journal of Human Evolution*, *65*, 79–92.

Pablos, A., Martínez, I., Lorenzo, C., Sala, N., Gracia-Téllez, A., & Arsuaga, J. L. (2014). Human calcanei from the Middle Pleistocene site of Sima de los Huesos (Sierra de Atapuerca, Burgos, Spain). *Journal of Human Evolution*, *76*, 63–76.

Pablos, A., Pantoja-Pérez, A., Martínez, I., Lorenzo, C., & Arsuaga, J. L. (2017). Metric and morphological analysis of the foot in the Middle Pleistocene population of Sima de los Huesos (Sierra de Atapuerca, Burgos, Spain). *Quaternary International*, *433*, 103–113.

Pablos, A., Sala, N., & Arribas, A. (2018). Taxonomic reassignment of the Paleolithic human navicular from Cueva de los Torrejones (Guadalajara, Spain). *Archaeological and Anthropological Sciences*, *10*, 1867–1880.

Pantoja-Pérez, A., Martínez, I., & Arsuaga, J. L. (2015). Metric analysis of the Sima de los Huesos crania. In R. M. Quam & J. L. Arsuaga (Eds.), *84th Annual Meeting of the American Association of Physical Anthropologists* (p. 247). American Association of Physical Anthropologists (AAPA).

Pantoja-Pérez, A., Sala, N., Arsuaga, J. L., Pablos, A., & Martínez, I. (2016). Virtual assessment for the study of the cranial fractures. Application to the Sima de los Huesos hominin crania. In *6th annual meeting of the European Society for the Study of Human Evolution (ESHE)* (p. 179). European Society for the Study of Human Evolution (ESHE).

Pearson, O. M., Pablos, A., Rak, Y., & Hovers, E. (2020). A partial Neandertal foot from the Late Middle Paleolithic of Amud cave, Israel. *PaleoAnthropology*, *2020*, 98–125.

Pearson, O. M., Royer, D. F., Grine, F. E., & Fleagle, J. G. (2008). A description of the Omo I postcranial skeleton, including newly discovered fossils. *Journal of Human Evolution*, *55*, 421–437.

Peckmann, T. R., Orr, K., Meek, S., & Manolis, S. K. (2015). Sex determination from the talus in a contemporary Greek population using discriminant function analysis. *The Journal of Forensic and Legal Medicine*, *33*, 14–19.

Pomeroy, E., Mirazon Lahr, M., Crivellaro, F., Farr, L., Reynolds, T., Hunt, C. O., & Barker, G. (2017). Newly-discovered Neanderthal remains from Shanidar Cave, Iraqi Kurdistan, and their attribution to Shanidar 5. *Journal of Human Evolution*, *11*, 102–118.

Rafter, J. A., Abell, M. L., & Braselton, J. P. (2002). Multiple comparison methods for means. *SIAM Review*, *44*, 259–278.

Raichlen, D. A., Armstrong, H., & Lieberman, D. E. (2011). Calcaneus length determines running economy: Implications for endurance running performance in modern humans and Neandertals. *Journal of Human Evolution*, *60*, 299–308.

Rhoads, J. G., & Trinkaus, E. (1977). Morphometrics of the Neandertal talus. *American Journal of Physical Anthropology*, *46*, 29–43.

Rodríguez, L., Carretero, J. M., García-González, R., & Arsuaga, J. L. (2018). Cross-sectional properties of the lower limb long bones in the Middle Pleistocene Sima de los Huesos sample (Sierra de Atapuerca, Spain). *Journal of Human Evolution*, *117*, 1–12.

Rodríguez, L., Carretero, J. M., García-González, R., Lorenzo, C., Gómez-Olivencia, A., Quam, R., Martínez, I., Gracia-Téllez, A., & Arsuaga, J. L. (2016). Fossil hominin radii from the Sima de los Huesos Middle Pleistocene site (Sierra de Atapuerca, Spain). *Journal of Human Evolution*, *90*, 55–73.

Rodríguez, L., García-González, R., Arsuaga, J. L., & Carretero, J.-M. (2024a). Exploring the morphology of adult tibia and fibula from Sima de los Huesos site in sierra de Atapuerca, Burgos, Spain. *The Anatomical Record*. https://doi.org/10.1002/ar.25336

Rodríguez, L., García-González, R., Arsuaga, J. L., & Carretero, J.-M. (2024b). Uncovering the adult morphology of

the forearm bones from the Sima de los Huesos Site in Atapuerca (Spain), with comments on biomechanical features. *The Anatomical Record*. https://doi.org/10.1002/ar.25281

Ryan, T. M., & Shaw, C. N. (2015). Gracility of the modern *Homo sapiens* skeleton is the result of decreased biomechanical loading. *Proceedings of the National Academy of Sciences of the United States of America*, *112*, 372–377.

Sala, N., Algaba, M., Gómez-Olivencia, A., Pablos, A., Bonmatí, A., Rodríguez, L., García, R., & Arsuaga, J. L. (2013). Nuevos restos humanos procedentes de la Cueva de la Zarzamora (Segovia, España). *Munibe Antropologia-Arkeologia*, *64*, 105–116.

Sala, N., Arsuaga, J. L., Martínez, I., & Gracia-Téllez, A. (2015). Breakage patterns in Sima de los Huesos (Atapuerca, Spain) hominin sample. *Journal of Archaeological Science*, *55*, 113–121.

Sala, N., Arsuaga, J. L., Pantoja-Pérez, A., Pablos, A., Martínez, I., Quam, R. M., Gómez-Olivencia, A., Bermúdez de Castro, J. M., & Carbonell, E. (2015). Lethal interpersonal violence in the Middle Pleistocene. *PLoS One*, *10*, e0126589.

Sala, N., Martínez, I., Lorenzo, C., García, R., Carretero, J. M., Rodríguez, L., Gómez-Olivencia, A., Aranburu, A., García, N., Quam, R., Gracia, A., Ortega, M. C., & Arsuaga, J. L. (2024). Taphonomic skeletal disturbances in the Sima de los Huesos postcranial remains. *The Anatomical Record*. https://doi.org/10.1002/ar.25197

Sala, N., Pantoja-Pérez, A., Arsuaga, J. L., Pablos, A., & Martínez, I. (2016). The Sima de los Huesos crania: Analysis of the cranial breakage patterns. *Journal of Archaeological Science*, *72*, 25–43.

Sala, N., Pantoja-Pérez, A., Gracia, A., & Arsuaga, J. L. (2024). Taphonomic-forensic analysis of the hominin skulls from the Sima de los Huesos. *The Anatomical Record*. https://doi.org/10.1002/ar.24883

Saldías, E., Malgosa, A., Jordana, X., & Isidro, A. (2016). Sex estimation from the navicular bone in Spanish contemporary skeletal collections. *Forensic Science International*, *267*, 229.e1–229.e6.

Shang, H., & Trinkaus, E. (2010). *The early modern human from Tianyuan Cave, China* Anthropology Series: no 14. Texas A&M University Press.

Simpson, S. W., Quade, J., Levin, N. E., Butler, R., Dupon-Nivet, G., Everett, M., & Semaw, S. (2008). A female *Homo erectus* pelvis from Gona, Ethiopia. *Science*, *322*, 1089–1092.

Sokal, R. R., & Rohlf, J. (2003). *Biometry. The principles and practice of statistics in biological research* (3rd ed.). W.H. Freeman and Company.

Sorrentino, R., Carlson, K. J., Bortolini, E., Minghetti, C., Feletti, F., Fiorenza, L., Frost, S., Jashashvili, T., Parr, W., Shaw, C., Su, A., Turley, K., Wroe, S., Ryan, T. M., Belcastro, M. G., & Benazzi, S. (2020). Morphometric analysis of the hominin talus: Evolutionary and functional implications. *Journal of Human Evolution*, *142*, 102747.

Sorrentino, R., Stephens, N. B., Carlson, K. J., Figus, C., Fiorenza, L., Frost, S., Harcourt-Smith, W., Parr, W., Saers, J., Turley, K., Wroe, S., Belcastro, M. G., Ryan, T. M., & Benazzi, S. (2020). The influence of mobility strategy on the modern human talus. *American Journal of Physical Anthropology*, *171*, 456–469.

Sorrentino, R., Stephens, N. B., Marchi, D., DeMars, L. J. D., Figus, C., Bortolini, E., Badino, F., Saers, J. P. P., Bettuzzi, M., Boschin, F., Capecchi, G., Feletti, F., Guarnieri, T., May, H., Morigi, M. P., Parr, W., Ricci, S., Ronchitelli, A., Stock, J. T., … Benazzi, S. (2021). Unique foot posture in Neanderthals reflects their body mass and high mechanical stress. *Journal of Human Evolution*, *161*, 103093.

Steele, D. G. (1976). The estimation of sex on the basis of the talus and calcaneus. *American Journal of Physical Anthropology*, *45*, 581–588.

Trinkaus, E. (1975). *A functional analysis of the Neandertal foot* (p. 533). Faculty of the Graduate school of Arts and Sciences, University of Pennsylvania.

Trinkaus, E. (1983a). Functional aspects of Neandertal pedal remains. *Foot & Ankle*, *3*, 377–390.

Trinkaus, E. (1983b). *The Shanidar Neandertals*. Academic Press.

Trinkaus, E. (2005). Early modern humans. *Annual Review of Anthropology*, *34*, 207–230.

Trinkaus, E. (2015). The appendicular skeletal remains of Oberkassel 1 and 2. In L. Giemsch & R. W. Schmitz (Eds.), *The late glacial burial from Oberkassel revisited* (pp. 75–132). Verlag Phillip von Zabern.

Trinkaus, E. (2016). *The Krapina human postcranial remains: Morphology, morphometrics and paleopathology*. FF Press.

Trinkaus, E., Buzhilova, A. P., Mednikova, M. B., & Dobrovolskaya, M. V. (2014). *The people of Sunghir: Burials, bodies, and behavior in the earlier Upper Paleolithic*. Oxford University Press.

Trinkaus, E., Thibeault, A., & Villotte, S. (2021). Disentangling Cro-Magnon: The pedal remains. *Journal of Archaeological Science: Reports*, *40*, 103228.

Trinkaus, E., Wotjal, P., Wilczyński, J., Sázelová, S., & Svoboda, J. (2017). Palmar, patellar and pedal human remains from Pavlov. *PaleoAnthropology*, *2017*, 73–101.

Vandermeersch, B. (1981). *Les hommes fossiles de Qafzeh (Israel)*. CNRS.

Vidal, C. M., Lane, C. S., Asrat, A., Barfod, D. N., Mark, D. F., Tomlinson, E. L., Tadesse, A. Z., Yirgu, G., Deino, A., Hutchison, W., Mounier, A., & Oppenheimer, C. (2022). Age of the oldest known *Homo sapiens* from eastern Africa. *Nature*, *601*, 579–583.

Will, M., Pablos, A., & Stock, J. T. (2017). Long-term patterns of body mass and stature evolution within the hominin lineage. *Royal Society Open Science*, *4*, 171339.

How to cite this article: Pablos, A., & Arsuaga, J. L. (2024). Tarsals from the Sima de los Huesos Middle Pleistocene site (Atapuerca, Burgos, Spain). *The Anatomical Record*, 1–30. https://doi.org/10.1002/ar.25425